HHS Public Access

Author manuscript

*Metab Brain Dis*. Author manuscript; available in PMC 2016 April 01.

Published in final edited form as:

*Metab Brain Dis*. 2015 April ; 30(2): 411–426. doi:10.1007/s11011-014-9550-3.

# Ablation of matrix metalloproteinase-9 gene decreases cerebrovascular permeability and fibrinogen deposition post traumatic brain injury in mice

**Nino Muradashvili, MD.**[1], **Richard L. Benton, PhD.**[2], **Kathryn E. Saatman, Ph.D.**[3], **Suresh C. Tyagi, PhD.**[1], and **David Lominadze, PhD.**[1,4]

[1]Department of Physiology and Biophysics, University of Louisville, School of Medicine, Louisville, KY

[2]Department of Anatomical Sciences and Neurobiology and Kentucky Spinal Cord Injury Research Center (KSCIRC), University of Louisville, School of Medicine, Louisville, KY

[3]Department of Physiology and Neurosurgery and Spinal Cord & Brain Injury Research Center (SCoBIRC), University of Kentucky, Lexington, KY, USA

## Abstract

Traumatic brain injury (TBI) is accompanied with enhanced matrix metalloproteinase-9 (MMP-9) activity and elevated levels of plasma fibrinogen (Fg), which is a known inflammatory agent. Activation of MMP-9 and increase in blood content of Fg (i.e. hyperfibrinogenemia, HFg) both contribute to cerebrovascular disorders leading to blood brain barrier disruption. It is well-known that activation of MMP-9 contributes to vascular permeability. It has been shown that at an elevated level (i.e. HFg) Fg disrupts blood brain barrier. However, mechanisms of their actions during TBI are not known. Mild TBI was induced in wild type (WT, C57BL/6J) and MMP-9 gene knockout ($Mmp9^{-/-}$) homozygous, mice. Pial venular permeability to fluorescein isothiocyanate-conjugated bovine serum albumin (FITC-BSA) in pericontusional area was observed 14 days after injury. Mice memory was tested with a novel object recognition test. Increased expression of Fg endothelial receptor intercellular adhesion protein-1 and formation of caveolae were associated with enhanced activity of MMP-9 causing an increase in pial venular permeability. As a result, an enhanced deposition of Fg and cellular prion protein ($PrP^C$) were found in pericontusional area. These changes were attenuated in $Mmp9^{-/-}$ mice and were associated with lesser loss of short-term memory in these mice than in WT mice. Our data suggest that mild TBI-induced increased cerebrovascular permeability enhances deposition of Fg-$PrP^C$ and loss of memory, which is ameliorated in the absence of MMP-9 activity. Thus, targeting MMP-9 activity and blood level of Fg can be a possible therapeutic remedy to diminish vasculo-neuronal damage after TBI.

[4]**Corresponding Author**: David Lominadze, Ph. D., University of Louisville, Dept. of Physiology & Biophysics, School of Medicine, Bldg. A, Room 1115, 500 South Preston Street, Louisville, KY 40202, Phone (502) 852-4902, Fax (502) 852-6239, david.lominadze@louisville.edu.

**Keywords**

Caveolae; cellular prion protein ($PrP^C$); cerebrovascular permeability; fibrinogen; macromolecular leakage; memory loss

## Introduction

Traumatic brain injury (TBI) is a major cause of death and disability, for which only supportive care is the most effective treatment. It is well known that besides the ruptured vessels in the injured area after TBI, cerebral vessels in the pericontusional region, which some define as an injury penumbra (Choo et al. 2013; Schwarzmaier et al. 2010), have an increased permeability (Shlosberg et al. 2010). TBI (Chhabra et al. 2010; Pahatouridis et al. 2010; Sun et al. 2011; Mansoor et al. 1997) as well as other inflammatory pathologies such as stroke (D'Erasmo et al. 1993; del Zoppo et al. 2009) and hypertension (Letcher et al. 1981; Lominadze et al. 1998) are accompanied with elevated blood content of fibrinogen (Fg), i.e. hyperfibrinogenemia (HFg). While Fg at the normal concentration (~2 mg/ml) has no discernible effects, at elevated levels (Fg level of ≥ 4 mg/ml, i.e. HFg) it is considered not only a marker of inflammation (Ross 1999) and a high risk factor for cardiovascular diseases (Ernst and Resch 1993), but also a cause of inflammatory responses (Tyagi et al. 2008; Patibandla et al. 2009; Kerlin et al. 2004; Lominadze et al. 2010; Muradashvili et al. 2012a).

One of the indications of inflammation is an increase in vascular permeability, which results in leakage of plasma substances and proteins out of the blood stream and their deposition in subendothelial matrix (SEM) and interstitium (Mehta and Malik 2006). While arteries and capillaries are practically impermeable to proteins, venules are the main site of protein leakage (Granger and Senchenkova 2010). These alterations that lead to accumulation of plasma proteins in SEM and interstitium cause edema and exacerbate complications of blood circulation during vascular diseases (Lominadze et al. 2010; Mehta and Malik 2006). Blood cells and plasma components may pass through the endothelial cell (EC) barrier via paracellular and transcellular pathways (Mehta and Malik 2006; Simionescu et al. 2009). Movement of plasma macromolecules via paracellular pathways occurs between the ECs and involves alterations in junction proteins (Mehta and Malik 2006). During the transvascular transport of proteins, transcytosis occurs across the ECs and involves caveolae, caveolae generated transendothelial channels, and fenestrae (Simionescu et al. 2009). The combination and the functional balance of paracellular and transcellular pathways govern the net extravascular transport of macromolecules in microvessels. However, a prevailing role of one or the other pathway in disruption of blood brain barrier (BBB) during various pathologies (e.g. TBI) is not clear.

One of the main components of the caveolae wall is caveolin-1 (Cav-1) (Yu et al. 2006). Plasmalemmal vesicle associated protein-1 (PV-1) is an integral membrane-associated protein of caveolae found in fenestrated endothelia and transendothelial channels (Carson-Walter et al. 2005; Hnasko et al. 2002; Stan et al. 1999). It is considered a functional biomarker for altered vascular permeability following the central nervous system trauma (Mozer et al. 2010) and disruption of BBB (Shue et al. 2008). Expression of PV-1 is

associated with caveolae formation (Mozer et al. 2010; Carson-Walter et al. 2005; Hnasko et al. 2002; Stan et al. 1999).

Apart from its key role in controlling blood loss following vascular injury, Fg extravasates at sites of increased vascular permeability (Tyagi et al. 2008) where it is immobilized and then converted to fibrin (Rybarczyk et al. 2003). It has been shown that undegraded Fg dose-dependently increases EC layer permeability to proteins and itself leaks through the EC layer (Tyagi et al. 2008). Others reported that undegraded Fg deposits in SEM (Sahni et al. 2009) leading to vascular remodeling. These findings emphasize a new role of Fg indicating its strong involvement in microvascular permeability and remodeling during various diseases associated with increased blood content of Fg (e.g. TBI).

Matrix metalloproteinases (MMPs), zinc-dependent endoproteinases expressed in ECs (Fernandez-Patron et al. 2001), are involved in both physiological and pathological processes in brain (Rosell et al. 2005; Rosell et al. 2006). It has been shown that blood content of MMP-9, the most abundant MMP, increases after TBI (Mori et al. 2002; Wang et al. 2000; Grossetete et al. 2009). Activation of MMP-9 involves extracellular signal-regulated kinase (ERK) signaling (Mori et al. 2002). This finding coincides with data indicating that increased binding of Fg to its endothelial surface receptor intercellular adhesion molecule-1 (ICAM-1) activates ERK (Sen et al. 2009) and is accompanied by an increased activity of MMP-9 (Muradashvili et al. 2012a), increases EC layer (Tyagi et al. 2008) and cerebrovascular permeability (Muradashvili et al. 2012a). It has been shown that activation of MMP-9 plays an important role in formation of brain edema after injury (Shigemori et al. 2006; Yamaguchi et al. 2007; Wang et al. 2000) and affects motor outcome (Wang et al. 2000). However, mechanisms of these effects and role of MMP-9 in cerebrovascular permeability and loss of memory after TBI still are not clear.

Memory impairment, particularly loss of short-term memory, is one of the problems of people with head injury (Cernich et al. 2010). Strong association of Amyloid beta (Aβ) peptide with Fg was linked to severity of Alzheimer disease (AD) (Ahn et al. 2010). It has been shown that axonal Aβ accumulation was accelerated in mice after cortical contusion injury (CCI) (Tran et al. 2011) and a strong connection between the Aβ pathology and loss of memory after TBI has been suggested (Johnson et al. 2010). However, some studies indicate that content of Aβ has limited effect on memory and point to a greater role of cellular prion protein ($PrP^C$) (Gimbel et al. 2010; Chung et al. 2010). Other studies suggest that the receptor for Aβ42 oligomer has deleterious effects on synaptic plasticity is $PrP^C$ (Lauren et al. 2009). It was shown that Fg interacts with non-digested $PrP^{Sc}$ (Fischer et al. 2000). Therefore, it is possible that formation of Fg-$PrP^C$ complex is involved in neurodegeneration after TBI.

It is well known that pial vessels are the resistance vessels that control global blood supply to the brain, while the intraparenchymal vessels are involved in the regulation of local cerebral blood flow (Cohen et al. 1996). Recently, it has been clearly shown that TBI causes significant changes in pial and parenchymal vessels altering their morphology and function (Sangiorgi et al. 2013). Thus, the primary injury caused by a head trauma affects pial vessels that are origins of perforating vessels. In addition, it has been shown that content of Fg

increases after local vascular injury (del Zoppo et al. 2009) and TBI (Chhabra et al. 2010; Sun et al. 2011; Pahatouridis et al. 2010). Therefore, it becomes imperative to investigate role of increased blood content of Fg in pial microvessels of pericontusional area after head injury. The present study aims to define role of Fg and MMP-9 activity, and their novel interaction with $PrP^C$, in cerebral pial microvascular permeability changes, leading to vasculo-neuronal disorders (Muradashvili and Lominadz 2013) that affect short-term memory after TBI.

## Materials and Methods

### Reagents and antibodies

Polyclonal rabbit anti-human Fg antibody was from Dako (Carpinteria, CA). Purified antibody against mouse ICAM-1 (CD54 - clone: YN1/1.7.4; Isotype: Rat IgG2b,κ) was obtained from BioLegend (San Diego, CA). Purified mouse anti phospho-caveolin-1 (pY14) was purchased from BD Biosciences (San Diego, CA). Rat anti-mouse PV-1 monoclonal antibody (clone: MECA-32; Isotype: IgG2a) was from AbD Serotec (Raleigh, NC). Polyclonal antibody against Cav-1 was obtained from Novus Biological (Littleton, CO). DQ gelatin, 1,10-phenanthroline,monohydrate, and secondary antibodies conjugated with Alexa-Fluor 488, Alexa-Fluor 594, or Alexa-Fluor 647 were purchased from Invitrogen (Carlsbad, CA). Monoclonal anti-Prion protein was from Sigma Aldrich Chemicals Co. (St. Louis, MO). 4,6-diamidino-2-phenyl-indole HCl (DAPI) were from Santa Cruz Biotechnology (Santa Cruz, CA). Normal Donkey Serum (NDS) was purchased from Jackson ImmunoResearch (West Grove, PA). Tetramethylrhodamine β-isothiocyanate (TRITC)- or fluorescein isothiocyanate (FITC)-conjugated Lycopersicon esculentum agglutinin (LEA) tomato lectin was from Vector laboratories (Burlingame, CA). Artificial cerebrospinal fluid (CSF) was purchased from Harvard Apparatus (Holliston, MA).

### Animals

In accordance of National Institute of Health Guidelines for animal research, all animal procedures for these experiments were reviewed and approved by the Institutional Animal Care and Use Committee of the University of Louisville.

Male wild-type (WT) C57BL/6J and MMP-9 gene knockout ($Mmp9^{-/-}$) homozygous (FVB.Cg-*Mmp9*$^{tm1Tvu}$/J; Stock Number: 004104) and its control FVB (FVB/NJ; Stock Number 001800) mice were obtained from the Jackson Laboratory (Bar Harbor, ME). For genotyping of $Mmp9^{-/-}$ mice, DNA was extracted from the tail tip of mice and was amplified by polymerase chain reaction (PCR) using the specific primer sequences according to the protocol described (Muradashvili et al. 2012a).

### Cortical contusion injury

Twelve-week old mice (26–30 g) were anesthetized with 2.5 % isoflurane, heads were shaved and they were placed in a stereotaxic frame (Kopf, Tujunga, CA). Isoflurane was delivered by a nose cone (Kopf). After exposing the skull with midline incision, a 4 mm diameter cranial window, centered at −2.5 mm bregma and 2.75 mm lateral to the midline over the left hemisphere was made without disturbing dura mater (Muradashvili et al.

2012a). During drilling, the cranium was continuously irrigated with phosphate buffered saline (PBS) at room temperature (RT). The impactor device (TBI 0310, Precision Systems & Instrumentation, Fairfax Station, VA) with 2 mm diameter flat tip was set to deliver an impact (0.5 mm impact depth, 3.5 m/s velocity, 500 ms simulation duration) to the cortical surface known to cause a mild-to-moderate injury (Pleasant et al. 2011). After injury Surgiseal (Johnson & Johnson) was laid on the dura, the skull cap was replaced, and the skin was sutured. The mice were placed on a heating pad to maintain normal body temperature until they were fully awake and returned to their home cages. In control (Sham-injured) group, craniotomy was performed, dura was covered with Surgiseal, the skull cap was replaced, and the skin was sutured. After recovery, mice were divided in two groups: one group of mice was selected for experimentation (cerebrovascular leakage) and another for tissue sample analyses 14 days after CCI. Additional group of WT and Mmp9−/− mice that did not underwent any surgery were used as additional controls to rule out possible effects of sham-injury in animals.

## Microvascular leakage observation

CCI-induced changes in pial venular permeability were observed according to the method described (Lominadze et al. 2006; Muradashvili et al. 2012b; Muradashvili et al. 2012a). Briefly, the animals were anesthetized with sodium pentobarbital (70 mg/kg, intraperitoneally). The trachea was cannulated to maintain a patent airway and animals were placed on heating pad to maintain body temperature at 37°C±1°C. Mean arterial blood pressure and heart rate were continuously monitored through a left carotid artery cannula (polyethylene tubing PE-10) connected to a transducer and a blood pressure analyzer (CyQ 103/302, Cybersense, Lexington, KY, USA). The skull cap was removed and the cranial window was extended using the micro-drill (Harvard Apparatus, Holliston, MA). The surface of the exposed pial circulation was continuously superfused with CSF. Constant temperature (37°C) of CSF was maintained by dual automatic temperature controller (Warner Instrument Corporation, Hamden, CT, USA). Mice were positioned on the stage of an Olympus BXG61WI microscope (Olympus, Tokyo, Japan) so that the exposed pial circulation could be observed by epi-illumination. Following the surgical preparation and preceding each experiment, there was a 30 min equilibration period. Before each experiment, autofluorescence of the observed area was recorded over a standard range of camera gains. FITC (300 μg/ml)-conjugated BSA (FITC-BSA, a total volume 120 μl) was infused through the carotid artery cannulation with a syringe pump (Harvard Apparatus, Holliston, MA) at 40 μl/min speed and allowed to circulate for 5 min (Lominadze et al. 2006; Muradashvili et al. 2012b; Muradashvili et al. 2012a).

Pial venular permeability was studied in pericontusional area at least 200 μm away from the injury perimeter (Fig. 1a). In littermate, sham-injured mice the observed area was at about the same location (relative to the cranial window) as in mice with CCI (Fig. 1a). The presence of unaltered blood flow in the microvessels located in pericontusional area was confirmed at the beginning of the experimentation. Venules were identified by observing the topology of the pial circulation and blood flow direction. Images of the selected third-order venular segments were recorded and used as baseline. After obtaining the baseline reading, images of the selected venular segments were recorded after 60 min. The area of interest

was exposed to blue (488 nm) light for 10–15 sec. The microscope images were acquired by an electron-multiplying charge-coupled device camera (Quantem 512SC, Photometrics, Tucson, AZ) and image acquisition system (Slidebook 5.0, Intelligent Imaging Innovations, Inc., Philadelphia, PA). The camera output was standardized with a 50 ng/ml fluorescein diacetate standard (Estman Kodak, Rochester, NY) for each experiment. The lamp power and camera gain settings were held constant during experiments, and the camera response was verified to be linear over the range used for these acquisitions. The magnification of the system with Olympus 10×/0.40 (UPlanSApo) objective was determined with a stage micrometer and vessel diameters were measured with the Slidebook 5.0.

Images of the pial venular circulation were analyzed by image analysis software (Image-Pro Plus 6.3, Media Cybernetics, Bethesda, MD) (Muradashvili et al. 2012b). Briefly, in each image, a Line Profile probe (LPP) was positioned across the venule stretching far to interstitium (Muradashvili et al. 2012b). Fluorescence intensity profile along this LPP allowed us to define vascular and interstitial interface with high precision (Muradashvili et al. 2012b). Then a 25 μm length LPP was positioned in the interstitium adjacent to a venular wall and in the middle of the venule parallel to the blood stream. Mean fluorescence intensities of FITC were measured 10 min (baseline) and 1 hour after infusion of the tracer. Leakage of BSA-FITC to interstitium was assessed by changes in the ratio of fluorescence intensity in the interstitium to that inside the venule. The results were averaged for each experimental group and presented as percent of baseline. The diameter of each venule under observation was also measured.

### Immunohistochemistry

In separate series of experiments contused or sham-injured mice were infused with FITC- or TRITC-conjugated LEA via the carotid cannulation to fluorescently label carbohydrate moieties on the intravascular endothelial surface (Muradashvili et al. 2012a). Animals were sacrificed with an anesthetic (pentobarbital) overdose, infused immediately with PBS and then with 4% paraformaldehyde solution through the left ventricle for exsanguination. The cranium was opened and the brain was removed and placed in 4% paraformaldehyde solution overnight and then kept in 30% Sucrose for 3 days. Mouse brain tissue immunohistochemistry was done according to the described method (Muradashvili et al. 2012a). Brain samples were mounted in protective matrix (Polyscience, Inc, Warrington, PA) and cryosectioned on the coronal plane using a Leica CM 1850 Cryocut (Bannockburn, IL). Fifteen μm thick slices were thaw-mounted on charged microscope slides (VWR, West Chester, PA) and stored at −80°C. Prior to immunostaining, slides were kept at −20°C overnight, and then warmed at 37°C for 20 min and mounting matrix was removed. The sections were post-fixed in ice-cold 100% methanol for 10 min, washed three times in Tris buffered saline (TBS) and blocked for non-specific epitope binding in 0.1% TritonX-100 TBS (TBS-T), 0.5% BSA and 10% NDS for 1h at RT.

Immunohistochemistry and laser-scanning confocal microscopy were used to detect expression of ICAM-1, Cav-1, PV-1, co-localization of Cav-1 and PV-1 (markers of caveolae), pCav-1, deposition of Fg, $PrP^C$, and formation of Fg-$PrP^C$ complex. These variables were observed in the area of pial vasculature located at least 200 μm away from

the injury and no more than 200 μm away from the brain surface (Fig. 2a). As a marker of caveolae formation, co-localization of Cav-1 and PV-1 and phosphorylation of Cav-1 as a possible indicator for Cav-1 signaling have been shown (Muradashvili et al. 2013). Off-line image analysis software (Image-Pro Plus) was used to assess expression of ICAM-1 and formations of caveolae or Fg-$PrP^C$ complex in bran vessels or their SEM (respectively). Fluorescence intensity was measured in the area of interest (AOI) placed along the vessel wall and normalized per length of the respective vascular segment. For each experimental group, 3–4 brain slices were analyzed. In each brain slice, three to five vessels were analyzed. Fluorescence intensity in 6 randomly placed constant size AOIs were measured. The results were averaged for each experimental group and values were presented as fluorescence intensity units (FIU).

### Western blot analysis

At the end of the experiments, blood was collected and plasma content of Fg was assessed by Western blot analysis. Equal volume (30 μl) of plasma protein from each animal group were loaded onto 10% SDS-PAGE gels and electrophoresed under reducing conditions and then transferred onto nitrocellulose membranes. Non-specific sites on membranes were blocked with 5% non-fat dry milk in TBS-T and membranes were incubated with anti-Fg antibodies overnight at 4°C. Then, probing with appropriate secondary antibody for 2 hours at RT, the blots were developed using a BioRad Molecular Imager (ChemiDoc XRS+, Hercules, CA). The blots were analyzed with Image Pro Plus. A plasma level of β-actin, which has been shown to be a least altered plasma protein (Zhang et al. 2012), was used as loading control. The levels of Fg were assessed by measuring an integrated optical density (IOD) of its bands in each sample lane profile relative to the IOD of the respective β-actin band.

### In-tissue zymography

In separate set of experiments, gelatinolytic activity of MMPs was demonstrated by in-tissue zymography as described (Muradashvili et al. 2012a). Briefly, DQ-gelatin was used as a substrate while 1,10-phenanthroline, monohydrate, a general metalloproteinase inhibitor, was used as a negative control. Unfixed mouse brain (not infused with paraformaldehyde) cryostat sections (15-μm thick) were warmed at 37°C for 20 min. DQ-gelatin was dissolved in water to 1 mg/mL concentration according to the manufacturer's recommendation, placed on the sections, and incubated for 2 hours on a rotator at RT. Samples were incubated with DAPI for 10 min. After washing with PBS, the slides were covered with glass coverslips. Laser scanning confocal microscope (objective 60×) was used to capture the images. Fluorescence was detected with the excitation at 484 nm and emission at 512 nm. As during immunohistochemistry study, off-line image analysis was used to assess activity of MMPs. The fluorescence intensity (a measure of MMP activity) was measured in same size AOI in all experimental groups. For each experimental group, 3–4 brain slices were analyzed. In each brain slice, 5 to 6 vascular images were analyzed. Fluorescence intensity in 6 randomly placed AOIs was measured and normalized per vascular segment length. The results are averaged for each experimental group and presented as FIUs.

### Short-term memory assessment

Short-term memory of mice was assessed with a novel object recognition test (NORT) as described (Bevins and Besheer 2006; Lyon et al. 2012) using a Top Scan behavioral analyzing system (Version 3.00 by Clever System. Inc; Reston, VA). Briefly, after two days of acclimatization following transportation, the animals were acclimated during three days for 10 min twice a day being placed in an empty box. On the day of experiment, two similar objects were placed in the box. The animal was positioned at the mid-point of wall opposite to objects for 5 min. After an hour one of the objects was replaced with a novel (different shape and size) object and the animal was returned to the box for 3 min. The behavioral assessment was provided by calculating discrimination ratio (DR, time spent at the novel object/time spent at both objects; values above 0.5 were considered as positive). Low DR (lesser interest and time spent at the novel object) indicates an impairment of memory (Bevins and Besheer 2006).

### Data analysis

All data are expressed as mean ± standard error of the mean. The experimental groups were compared by one-way ANOVA. Two-way ANOVA was used to assess effects of genetic difference and cerebrovascular permeability, expression of ICAM-1, formation of caveolae (co-localization of Cav-1 and PV-1), phosphorylation of Cav-1, formation of Fg-$PrP^C$ complex (co-localization of deposited Fg and $PrP^C$), and changes in short-term memory. Effects were considered significant if $P < 0.05$, and a comparison of means (Tukey's multiple comparison test) was done for significant interactions. Differences in means were considered significant if $P < 0.05$.

## RESULTS

### FITC-BSA crossing of pial venular walls

Infusion of FITC-BSA did not affect diameters of observed pial venules in WT (41±4 μm before and 43±3 μm after infusion), $Mmp9^{-/-}$ (43±5 μm before and 45±4 μm after infusion), and FVB (45±4 μm before and 47±5 μm after infusion) mice. These results are consistent with other observations where infusion of 70–150 μl solution did not affect pail vascular diameters (Lominadze et al. 2006; Muradashvili et al. 2012a; Muradashvili et al. 2012b).

In WT mice, as in FVB mice, pial venular permeability was increased after CCI compared to that in respective sham-injured mice (Fig. 1b,c). Similarly, in $Mmp9^{-/-}$ mice, venular leakage of FITC-BSA was greater after CCI than that in littermate sham-injured mice (Fig. 1b,c). However, BSA crossing of pial venular walls in $Mmp9^{-/-}$ mice after CCI was significantly lesser than that in WT or FVB mice after CCI (Fig. 1b,c). Overall, permeability of pial venules in $Mmp9^{-/-}$ mice (after CCI or sham-injury) was lesser than that in respective groups of WT or FVB mice (Fig. 1b,c). Permeability of pial venules of sham WT mice (139 ± 8 % of baseline) was greater than that (115 ± 6 % of baseline) in sham $Mmp9^{-/-}$ mice, but was similar to that (138 ± 5 % of baseline) in sham FVB mice.

To determine relative changes in venular permeability after TBI, ratio of venular permeability after CCI to that in sham-injured mice in each group has been calculated. Pial

venular leakage to FITC-BSA after TBI in WT was 1.3 ± 0.001 - times higher than in WT-sham mice. This increase was greater than that (1.1 ± 0.01) in Mmp9$^{-/-}$ mice and was not different from that (1.33 ± 0.09) in FVB mice.

### Fg content in mouse plasma

In WT mice, CCI induced an increase in plasma Fg level compared to that in sham-injured mice (Fig. 1 inset). Similarly, in Mmp9$^{-/-}$ mice, Fg level was greater after CCI than that in littermate sham-injured mice (Fig. 1 inset). However, contents of Fg after CCI or sham-injury in Mmp9$^{-/-}$ mice were significantly lesser that those in respective groups of WT animals (Fig. 1 inset). After CCI, plasma content of Fg increased similarly in WT, Mmp9−/−, and FVB mice (Fig. 1 inset).

### ICAM-1 expression

Endothelial expression of ICAM-1 in brain cortical vessels was greater after CCI in WT mice than that after sham injury (Fig. 2). In Mmp9$^{-/-}$ mice, expression of endothelial ICAM-1 was also increased after CCI compared to that in littermate sham-injured mice (Fig. 2). However, expression of endothelial ICAM-1 in cortical vessels of Mmp9$^{-/-}$ mice was lesser than that in WT mice after CCI or sham injury (Fig. 2).

### Activity of MMP-9

TBI-induced activation of MMP-9 was shown by in-tissue zymography, which mainly detects activation of MMP-9 and MMP-2 (Muradashvili et al. 2012a). TBI increased activity of MMPs in both WT and Mmp9$^{-/-}$ mice (Fig. 3). However, activity of MMPs after CCI was greater in WT (Fig. 3; 14.8 ± 0.7 FIU) than in Mmp9$^{-/-}$ (Fig. 3; 9.2 ± 0.3 FIU) mice. The difference (5 ± 0.3 FIU) in activities of MMPs between WT and Mmp9$^{-/-}$ mice after TBI was solely determined by activity of MMP-9 and was greater than that (2 ± 0.1 FIU) in sham-operated mice.

### Expression of Cav-1and PV-1, caveolae formation, and Cav-1 phosphorylation after TBI

Expression of Cav-1 (Fig. 4a,b) and PV-1 (Fig. 4a,c) was increased after CCI in WT and Mmp9$^{-/-}$ mice. However, expression of these proteins was less in Mmp9$^{-/-}$ mice than in WT mice (Fig. 4a,b for Cav-1 and Fig. 4a,c for PV-1). Possible formation of caveolae was defined as co-localization of Cav-1 (red) and PV-1 (green) in mice cortical samples (Fig. 4a). Co-localization (yellow) of these proteins in brain cortical vessels of mice, which most likely indicates caveolae (Muradashvili et al. 2013), was increased in WT and Mmp9$^{-/-}$ mice after CCI in comparison to that in respective sham-injured groups (Fig. 4a). These results suggest that formation of caveolae most likely increases after CCI, but to a lesser extent in the absence of MMP-9 activity.

Phosphorylation of Cav-1 was greater in WT than in Mmp9$^{-/-}$ mice (Fig. 5). TBI-increased phosphorylation of Cav-1 in WT mice was greater than that in Mmp9$^{-/-}$ mice (Fig. 5) suggesting that possible formation of functional caveolae in endothelium of mouse brain cortical vessels may occur via Cav-1 signaling mechanism.

### Deposition of Fg and Fg-PrP$^C$ complex formation in brain cortical vessels

In WT mice, CCI-induced deposition of Fg in pericontusional area was increased compared to that in an area around the skull opening in sham-injured WT mice (Fig. 6a,b). Similarly, in Mmp9$^{-/-}$ mice, deposition of Fg in pericontusional area was greater than that in area of sham injury in littermate sham-injured mice (Fig. 6a,b). However, deposition of Fg in pericontusional area of Mmp9$^{-/-}$ mice was significantly less than that in WT mice (Fig. 6a,b). Overall, Fg deposition in cerebral cortex of Mmp9$^{-/-}$ mice (after CCI or sham-injury) was less than that in respective groups of WT mice (Fig. 6a,b). Deposition of Fg (Fig. 6a,b) and expression of PrP$^C$ (Fig. 6a,c) and number of objects with co-localized Fg and PrP$^C$ (Fig. 6a,d) suggesting a possible formation of Fg-PrP$^C$ complex were greater after CCI compared that to respective sham-injured mice in both animal groups. However, these changes were smaller in Mmp9$^{-/-}$ mice compared those in WT mice.

### Short-term memory

Short-term memory of mice was impaired after TBI in all WT, Mmp9$^{-/-}$, and FVB mice (Fig. 7). Although DRs in WT, Mmp9$^{-/-}$, and FVB were not different after CCI, they were less than those in respective sham-injured mice (Fig. 7). This decrease in short-term memory after CCI was smaller in Mmp9$^{-/-}$ mice than that in WT or FVB mice (Fig. 7). There were no differences in short-term memory level or its changes after CCI between WT and FVB mice (Fig. 7).

## Discussion

Our data indicate that brain injury-induced increase in vascular wall permeability in pericontusional area may cause neuronal impairment resulting in short-term memory changes. Thus, the main cause of possible neuronal damage leading to cognitive changes is alteration in vascular properties, particularly vascular permeability, and the resultant events. Therefore, to adequately define cause and effect after brain trauma or any cerebrovascular abnormality leading to neuronal impairment it is preferable to use a new term “vasculo-neuronal” damage. The term vasculo-neuronal-inflammatory triad has been coined by Zlokovic and Griffin to show that a pathological triad consisting of vascular damage, neuronal injury and/or neurodegeneration, and neuroinflammation is present in stroke and may other neurological disorders (Zlokovic and Griffin 2011). In the case of TBI, alterations in microvascular properties and microcirculation lead to changes in neuronal function and therefore, the sequence of events resembles the sequence defined by Zlokovic and Griffin (Zlokovic and Griffin 2011). Therefore, neuronal dysfunction after TBI that are initiated mainly from abnormalities associated with vasculature can be called a vasculo-neuronal disorder.

It is known that TBI is an inflammatory disease. Since blood content of Fg is increased during inflammation (D'Erasmo et al. 1993; Ross 1999; Sun et al. 2011; Davalos and Akassoglou 2012) we may conclude that TBI-induced inflammation causes an increase in blood content of Fg. This was confirmed by our data showing an increase in plasma level of Fg after TBI in all three mice groups. It has been demonstrated that at high level of Fg its binding to endothelial ICAM-1 is increased (Lominadze et al. 2005). In the present study we

showed that TBI induced an increase in expression of endothelial ICAM-1, which is a known endothelial surface receptor of Fg (Altieri et al. 1995; Plow et al. 2000). This can be a mechanism for an increased binding of Fg to vascular endothelium.

We found that activity of MMP-9 is increased after TBI suggesting that this enzyme can be involved in increase in cerebrovascular permeability. Elevation in blood level of Fg was shown to be associated with increased activity of MMP-9 (Muradashvili et al. 2012a). Combined, these results indicate a possible role of MMP-9 activity in increased cerebrovascular permeability after TBI.

It was found that enhanced binding of Fg to ECs alters EC structure (formation of filamentous actin) (Tyagi et al. 2008) and affects EC junction proteins (Patibandla et al. 2009). These events can be involved in an increase of cerebrovascular permeability and have a significant effect on vascular remodeling (such as Fg deposition in SEM) in brain vasculature during HFg (Lominadze et al. 2010; Muradashvili et al. 2011; Muradashvili et al. 2012a; Muradashvili et al. 2012b). On the other hand, during HFg, an increase in cerebrovascular permeability and particularly proteins crossing of vascular wall occurs via mainly the transcellular transport (Muradashvili et al. 2012b).

It is known that Cav-1 (Yu et al. 2006) and PV-1 (Carson-Walter et al. 2005; Hnasko et al. 2002; Stan et al. 1999) are associated with caveolae. We found that expressions of Cav-1 and PV-1 were increased after TBI. Most importantly, association of Cav-1 and PV-1 was increased after TBI. This association can be considered as a marker of functional caveolae formation (Muradashvili et al. 2013). Several laboratories have reported that phosphorylation of Cav-1 plays an essential role in the caveolae formation mechanisms (Hu et al. 2008; Sun et al. 2009; Wei et al. 2009; Parton et al. 1994; Minshall et al. 2000). Moreover, motility of caveolae is mediated by Cav-1 phosphorylation-dependent signaling events associated with binding of albumin to its endothelial receptor gp60 in caveolae (Minshall et al. 2000). In the present study, we found that permeability of pial venules was increased in pericontusional area after CCI. This increased venular permeability was correlated with an increased association of Cav-1 and PV-1 and with increased phosphorylation of Cav-1 indicating an increase in possible formation of functional caveolae as it was shown in other study (Muradashvili et al. 2013). However, expression of Cav-1, PV-1, their co-localization, and phosphorylation of Cav-1 were less in $Mmp9^{-/-}$ mice even after TBI. Smaller changes in these variables in $Mmp9^{-/-}$ mice after TBI were associated with lower cerebrovascular permeability. Combined, these results suggest that TBI-induced increase in blood content of Fg leads to an increased activation of ECs enhancing a protein transcytosis involving mainly caveolae-mediated transport pathway. Absence of MMP-9 most likely affects caveolar transcytosis decreasing Fg-to-ICAM-1 binding-induced endothelial activation and the resultant caveolar transcytosis. These data coincide with other results showing the correlation of enhanced blood level of Fg, MMP-9 activity, and caveolar transcytosis (Muradashvili et al., 2012a, Muradashvili et al., 2013).

Increased protein transcytosis after TBI leads to an accumulation of Fg in SEM, which was indicated by increased deposition of Fg in brain cortical samples. Subsequent possible binding of Fg (or already formed fibrin) to $PrP^C$ resulted in formation of Fg-$PrP^C$ complex.

This complex would most likely be more resistant to protein degradation in brain tissue. Since a role for $PrP^C$ in memory impairment is known (Gimbel et al. 2010; Chung et al. 2010), degradation-resistant Fg-$PrP^C$ complex could be involved in short-term memory impairment seen the present study. Recent data indicating a possible role of MMP-9 activity on memory loss after sever TBI (Hadass et al. 2013) confirm results of the present study. Lesser changes in memory after mild CCI in $Mmp9^{-/-}$ mice can be a result of lesser cerebrovascular permeability to Fg, which leads to a lesser accumulation of Fg in SEM and lesser formation of Fg-$PrP^C$ complex. The results showing that plasma level of Fg is increased in $Mmp9^{-/-}$ mice after CCI, indicate that lower cerebrovascular permeability in these mice can be a reason for the minimal formation of Fg-$PrP^C$ complex.

The results of the present study clarify mechanisms of TBI-induced formation of Fg-$PrP^C$ complex and the resultant loss in short-term memory. The schematic representation of these mechanisms is presented in Fig. 8. Overall, our data indicate a role of caveolae and their function in pial venular permeability suggesting a transcellular transport as a main protein transport pathway in cerebrovascular permeability after CCI. This protein transcytosis by caveolae is most likely mediated by Cav-1 signaling and involves activation of MMP-9. Precise molecular mechanism of MMP-9 activity action in formation of functional caveolae is still not clear. However, we have shown a strong association of MMP-9 activity with caveolar transcytosis after TBI. As a result, blood proteins such as albumin and Fg itself can cross pial venular wall and accumulate in SEM. This increased deposition of blood proteins in SEM would inevitably lead to edema formation. In addition, enhanced deposition of Fg on vascular wall and most importantly in SEM may create conditions susceptible to formation of Fg-$PrP^C$ complex. The formed complex, which has a high resistance to degradation, can contribute to short-term memory impairment. In addition, Fg immobilized in SEM can affect microglia and cause a significant rearrangement of their cytoskeleton and increase in cell size and phagocytic activity (Adams et al. 2007). Fg binds microglia via its receptor Mac-1 (Adams et al. 2007; Davalos and Akassoglou 2012). While studying Fg to Mac-1 binding, it has been shown that immobilized Fg and insoluble fibrin, but not soluble Fg, have been identified as physiological, high-affinity ligands for Mac-1 (Flick et al. 2004; Lishko et al. 2002). These results suggest that Fg that crossed vascular wall and deposited in SEM and brain tissue binds to microglia leading to the development of axonal damage (Davalos et al. 2012). Thus, increased blood content of Fg that occurs after TBI can be a mechanism for a vasculo-neuronal abnormality associated with brain trauma.

## Acknowledgments

Supported in part by NIH grants P30 GM-103507 (Pilot Project to D.L.), NS-084823 (to D.L. and S.C.T.), and NS-051568 (to S.C.T.)

## References

Adams RA, Bauer J, Flick MJ, Sikorski SL, Nuriel T, Lassmann H, Degen JL, Akassoglou K. The fibrin-derived γ377–395 peptide inhibits microglia activation and suppresses relapsing paralysis in central nervous system autoimmune disease. The Journal of Experimental Medicine. 2007; 204(3): 571–582. [PubMed: 17339406]

Ahn HJ, Zamolodchikov D, Cortes-Canteli M, Norris EH, Glickman JF, Strickland S. Alzheimer's disease peptide β-amyloid interacts with fibrinogen and induces its oligomerization. Proceedings of the National Academy of Sciences. 2010; 107(50):21812–21817.

Altieri DC, Duperray A, Plescia J, Thornton GB, Languino LR. Structural recognition of a novel fibrinogen gamma chain sequence (117–133) by intercellular adhesion molecule-1 mediates leukocyte-endothelium interaction. J Biol Chem. 1995; 270(2):696–699. [PubMed: 7822297]

Bevins RA, Besheer J. Object recognition in rats and mice: a one-trial non-matching-to-sample learning task to study 'recognition memory'. Nat Protocols. 2006; 1(3):1306–1311. doi:http://www.nature.com/nprot/journal/v1/n3/suppinfo/nprot.2006.205_S1.html.

Carson-Walter E, Hampton J, Shue E, Geynisman D, Pillai P, Sathanoori R, Madden S, Hamilton R, Walter K. Plasmalemmal vesicle associated protein-1 is a novel marker implicated in brain tumor angiogenesis. Clinical Cancer Research. 2005; 11(21):7643–7650. [PubMed: 16278383]

Cernich A, Kurtz S, Mordecai K, Ryan P. Cognitive rehabilitation in traumatic brain injury. Curr Treat Options Neurol. 2010; 12(5):412–423. [PubMed: 20842598]

Chhabra G, Rangarajan K, Subramanian A, Agrawal D, Sharma S, Mukhopadhayay A. Hypofibrinogenemia in isolated traumatic brain injury in Indian patients. Neurology India. 2010; 58(5):756–757. doi:DOI:10.4103/0028-3886: 72175. [PubMed: 21045504]

Choo AM, Miller WJ, Chen Y-C, Nibley P, Patel TP, Goletiani C, Morrison B, Kutzing MK, Firestein BL, Sul J-Y, Haydon PG, Meaney DF. Antagonism of purinergic signalling improves recovery from traumatic brain injury. Brain. 2013

Chung E, Ji Y, Sun Y, Kascsak R, Kascsak R, Mehta P, Strittmatter S, Wisniewski T. Anti-PrPC monoclonal antibody infusion as a novel treatment for cognitive deficits in an Alzheimer's disease model mouse. BMC Neuroscience. 2010; 11:130. [PubMed: 20946660]

Cohen ZVI, Bonvento G, Lacombe P, Hamel E. Serotonin in the regulation of brain microcirculation. Progress in Neurobiology. 1996; 50(4):335–362. [PubMed: 9004349]

D'Erasmo E, Acca M, Celi FS, Medici F, Palmerini T, Pisani D. Plasma fibrinogen and platelet count in stroke. Journal of Medicine. 1993; 24(2–3):185–191. [PubMed: 8409781]

Davalos D, Akassoglou K. Fibrinogen as a key regulator of inflammation in disease. Seminars In Immunopathology. 2012; 34(1):43–62. [PubMed: 22037947]

Davalos D, Kyu Ryu J, Merlini M, Baeten KM, Le Moan N, Petersen MA, Deerinck TJ, Smirnoff DS, Bedard C, Hakozaki H, Gonias Murray S, Ling JB, Lassmann H, Degen JL, Ellisman MH, Akassoglou K. Fibrinogen-induced perivascular microglial clustering is required for the development of axonal damage in neuroinflammation. Nat Commun. 2012; 3:1227. doi:http://www.nature.com/ncomms/journal/v3/n11/suppinfo/ncomms2230_S1.html. [PubMed: 23187627]

del Zoppo GJ, Levy DE, Wasiewski WW, Pancioli AM, Demchuk AM, Trammel J, Demaerschalk BM, Kaste M, Albers GW, Ringelstein EB. Hyperfibrinogenemia and functional outcome from acute ischemic stroke. Stroke. 2009; 40(5):1687–1691. [PubMed: 19299642]

Ernst E, Resch KL. Fibrinogen as a cardiovascular risk factor: a meta-analysis and review of the literature. Ann Intern Med. 1993; 118:956–963. [PubMed: 8489110]

Fernandez-Patron C, Zouki C, Whittal R, Chan JS, Davidge ST, Filep JG. Matrix metalloproteinases regulate neutrophil-endothelial cell adhesion through generation of endothelin-1[1–32]. The FASEB Journal. 2001; 15(12):2230–2240.

Fischer MB, Roeckl C, Parizek P, Schwarz HP, Aguzzi A. Binding of disease-associated prion protein to plasminogen. Nature. 2000; 408(6811):479–483. [PubMed: 11100730]

Flick MJ, Du X, Witte DP, Jirou x, kov xE, Mark xE, ta, Soloviev DA, Busuttil SJ, Plow EF, Degen JL. Leukocyte engagement of fibrin(ogen) via the integrin receptor αMβ2/Mac-1 is critical for host inflammatory response in vivo. The Journal of Clinical Investigation. 2004; 113(11):1596–1606. [PubMed: 15173886]

Gimbel DA, Nygaard HB, Coffey EE, Gunther EC, Laurén J, Gimbel ZA, Strittmatter SM. Memory impairment in transgenic Alzheimer mice requires cellular prion protein. The Journal of Neuroscience. 2010; 30(18):6367–6374. [PubMed: 20445063]

Granger, D.; Senchenkova, E. Colloquium Series on Integrated Systems Physiology: From Molecule to Function to Disease. San Rafael, CA: Morgan & Claypool Life Sciences; 2010. Inflammation and the Microcirculation.

Grossetete M, Phelps J, Arko L, Yonas H, Rosenberg G. Elevation of matrix metalloproteinases 3 and 9 in cerebrospinal fluid and blood in patients with severe traumatic brain injury. Neurosurgery. 2009; 65(4):702–708. [PubMed: 19834375]

Hadass O, Tomlinson BN, Gooyit M, Chen S, Purdy JJ, Walker JM, Zhang C, Giritharan AB, Purnell W, Robinson CR II, Shin D, Schroeder VA, Suckow MA, Simonyi AY, Sun G, Mobashery S, Cui J, Chang M, Gu Z. Selective inhibition of matrix metalloproteinase-9 attenuates secondary damage resulting from severe traumatic brain injury. PLoS ONE. 2013; 8(10):e76904. [PubMed: 24194849]

Hnasko R, McFarland M, Ben-Jonathan N. Distribution and characterization of plasmalemma vesicle protein-1 in rat endocrine glands. J Endocrinol. 2002; 175(3):649–661. [PubMed: 12475376]

Hu G, Vogel SM, Schwartz DE, Malik AB, Minshall RD. Intercellular Adhesion Molecule-1–Dependent Neutrophil Adhesion to Endothelial Cells Induces Caveolae-Mediated Pulmonary Vascular Hyperpermeability. Circulation Research. 2008; 102(12):e120–e131. [PubMed: 18511851]

Johnson VE, Stewart W, Smith DH. Traumatic brain injury and amyloid-[beta] pathology: a link to Alzheimer's disease? Nat Rev Neurosci. 2010; 11(5):361–370. [PubMed: 20216546]

Kerlin B, Cooley BC, Isermann BH, Hernandez I, Sood R, Zogg M, Hendrickson SB, Mosesson MW, Lord S, Weiler H. Cause-effect relation between hyperfibrinogenemia and vascular disease. Current Opinion in Hematology. 2004; 103(5):1728–1734.

Lauren J, Gimbel DA, Nygaard HB, Gilbert JW, Strittmatter SM. Cellular prion protein mediates impairment of synaptic plasticity by amyloid-[bgr] oligomers. Nature. 2009; 457(7233):1128–1132. doi:http://www.nature.com/nature/journal/v457/n7233/suppinfo/nature07761_S1.html. [PubMed: 19242475]

Letcher RL, Chien S, Pickering TG, Sealey JE, Laragh JH. Direct relationship between blood pressure and blood viscosity in normal and hypertensive subjects. Role of fibrinogen and concentration. The American Journal of Medicine. 1981; 70:1195–1202. [PubMed: 7234890]

Lishko VK, Kudryk B, Yakubenko VP, Yee VC, Ugarova TP. Regulated unmasking of the cryptic binding site foriIntegrin αMβ2 in the γC-domain of fibrinogen. Biochemistry. 2002; 41(43):12942–12951. [PubMed: 12390020]

Lominadze D, Dean WL, Tyagi SC, Roberts AM. Mechanisms of fibrinogen-induced microvascular dysfunction during cardiovascular disease. Acta Physiologica. 2010; 198(1):1–13. [PubMed: 19723026]

Lominadze D, Joshua IG, Schuschke DA. Increased erythrocyte aggregation in spontaneously hypertensive rats. AmJHypertens. 1998; 11:784–789.

Lominadze D, Roberts AM, Tyagi N, Tyagi SC. Homocysteine causes cerebrovascular leakage in mice. Am J Physiol Heart Circ Physiol. 2006; 290(3):H1206–H1213. [PubMed: 16258031]

Lominadze D, Tsakadze N, Sen U, Falcone JC, D'Souza SE. Fibrinogen- and fragment D-induced vascular constriction. American Journal of Physiology. 2005; 288(3):H1257–H1264. [PubMed: 15739255]

Lyon L, Saksida L, Bussey T. Spontaneous object recognition and its relevance to schizophrenia: a review of findings from pharmacological, genetic, lesion and developmental rodent models. Psychopharmacology. 2012; 220(4):647–672. [PubMed: 22068459]

Mansoor O, Cayol M, Gachon P, Boirie Y, Schoeffler P, Obled C, Beaufrère B. Albumin and fibrinogen syntheses increase while muscle protein synthesis decreases in head-injured patients. American Journal of Physiology - Endocrinology And Metabolism. 1997; 273(5):E898–E902.

Mehta D, Malik AB. Signaling mechanisms regulating endothelial permeability. Physiological Reviews. 2006; 86(1):279–367. [PubMed: 16371600]

Minshall RD, Tiruppathi C, Vogel SM, Niles WD, Gilchrist A, Hamm HE, Malik AB. Endothelial cell-surface gp60 activates vesicle formation and trafficking via G(i)-coupled Src kinase signaling pathway. The Journal of Cell Biology. 2000; 150(5):1057–1070. [PubMed: 10973995]

Mori T, Wang X, Aoki T, Lo EH. Downregulation of matrix metalloproteinase-9 and attenuation of edema via inhibition of ERK mitogen activated protein kinase in traumatic brain injury. Journal of Neurotrauma. 2002; 19(11):1411–1419. doi:doi:10.1089/089771502320914642. [PubMed: 12490006]

Mozer A, Whittemore S, Benton R. Spinal microvascular expression of PV-1 is associated with inflammation, perivascular astrocyte loss, and diminished EC glucose transport potential in acute SCI. Current Neurovascular Research. 2010; 7(3):238–250. [PubMed: 20590523]

Muradashvili N, Benton R, Tyagi S, Lominadz D. Elevated level of fibrinogen increases caveolae formation; Role of matrix metalloproteinase-9. Cell Biochemistry and Biophysics. 2013 [Epub ahead of print].

Muradashvili N, Lominadz D. Role of fibrinogen in cerebrovascular dysfunction after traumatic brain injury. Brain Injury. 2013; 27(13–14):1508–1515. [PubMed: 24063686]

Muradashvili N, Qipshidze N, Munjal C, Givvimani S, Benton RL, Roberts AM, Tyagi SC, Lominadze D. Fibrinogen-induced increased pial venular permeability in mice. Journal of Cerebral Blood Flow and Metabolism. 2012a; 32(1):150–163. [PubMed: 21989482]

Muradashvili N, Tyagi N, Tyagi R, Munjal C, Lominadze D. Fibrinogen alters mouse brain endothelial cell layer integrity affecting vascular endothelial cadherin. Biochemical and Biophysical Research Communications. 2011; 413(4):509–514. [PubMed: 21920349]

Muradashvili N, Tyagi R, Lominadze D. A dual-tracer method for differentiating transendothelial transport from paracellular leakage in vivo and in vitro. Frontiers in Physiology. 2012b; 3:166–172. [PubMed: 22754530]

Pahatouridis D, Alexiou G, Zigouris A, Mihos E, Drosos D, Voulgaris S. Coagulopathy in moderate head injury. The role of early administration of low molecular weight heparin. Brain Injury. 2010; 24(10):1189–1192. [PubMed: 20642324]

Parton RG, Joggerst B, Simons K. Regulated internalization of caveolae. The Journal of Cell Biology. 1994; 127(5):1199–1215. [PubMed: 7962085]

Patibandla PK, Tyagi N, Dean WL, Tyagi SC, Roberts AM, Lominadze D. Fibrinogen induces alterations of endothelial cell tight junction proteins. Journal of Cellular Physiology. 2009; 221(1): 195–203. [PubMed: 19507189]

Phillips PG, Birnby LM. Nitric oxide modulates caveolin-1 and matrix metalloproteinase-9 expression and distribution at the endothelial cell/tumor cell interface. American Journal of Physiology - Lung Cellular and Molecular Physiology. 2004; 286(5):L1055–L1065. [PubMed: 15064242]

Pleasant J, Carlson S, Mao H, Scheff S, Yang K, Saatman K. Rate of neurodegeneration in the mouse controlled cortical impact model is influenced by impactor tip shape: implications for mechanistic and therapeutic studies. Journal of Neurotrauma. 2011

Plow EF, Haas TA, Zhang L, Loftus J, Smith JW. Ligand binding to integrins. The Journal of Biological Chemistry. 2000; 275(29):21785–21788. [PubMed: 10801897]

Rosell A, Alvarez-Sabin J, Arenillas JF, Rovira A, Delgado P, Fernandez-Cadenas I, Penalba A, Molina CA, Montaner J. A matrix metalloproteinase protein array reveals a strong relation between MMP-9 and MMP-13 with diffusion-weighted image lesion increase in human stroke. Stroke. 2005; 36(7):1415–1420. [PubMed: 15947272]

Rosell A, Ortega-Aznar A, Alvarez-Sabin J, Fernandez-Cadenas I, Ribo M, Molina CA, Lo EH, Montaner J. Increased brain expression of matrix metalloproteinase-9 after ischemic and hemorrhagic human stroke. Stroke. 2006; 37(6):1399–1406. [PubMed: 16690896]

Ross R. Mechanisms of disease - Atherosclerosis - An inflammatory disease. New England Journal of Medicine. 1999; 340(2):115–126. [PubMed: 9887164]

Rybarczyk BJ, Lawrence SO, Simpson-Haidaris PJ. Matrix-fibrinogen enhances wound closure by increasing both cell proliferation and migration. Blood. 2003; 102(12):4035–4043. [PubMed: 12920033]

Sahni A, Arévalo MT, Sahni SK, Simpson-Haidaris PJ. The VE-cadherin binding domain of fibrinogen induces endothelial barrier permeability and enhances transendothelial migration of malignant breast epithelial cells. International Journal of Cancer. 2009; 125(3):577–584.

Sangiorgi S, De Benedictis A, Protasoni M, Manelli A, Reguzzoni M, Cividini A, Dell'Orbo C, Tomei G, Balbi S. Early-stage microvascular alterations of a new model of controlled cortical traumatic brain injury 3D morphological analysis using scanning electron microscopy and corrosion casting. Journal of Neurosurgery. 2013; 118(4):763–774. doi:doi:10.3171/2012.11.JNS12627. [PubMed: 23350772]

Schwarzmaier S, Kim S, Trabold R, Plesnila N. Temporal profile of thrombogenesis in the cerebral microcirculation after traumatic brain injury in mice. Journal of Neurotrauma. 2010; 27(1):121–130. [PubMed: 19803784]

Sen U, Tyagi N, Patibandla PK, Dean WL, Tyagi SC, Roberts AM, Lominadze D. Fibrinogen-induced endothelin-1 production from endothelial cells. AJP - Cell Physiology. 2009; 296(4):C840–C847. [PubMed: 19193866]

Shigemori, Y.; Katayama, Y.; Mori, T.; Maeda, T.; Kawamata, T. Matrix metalloproteinase-9 is associated with blood-brain barrier opening and brain edema formation after cortical contusion in rats. In: Hoff, JT.; Keep, RF.; Xi, G.; Hua, Y., editors. Wien: Springer-Verlag; 2006. p. 130-133.Brain Edema XIII, vol 96. Acta Neurochirurgica Supplement vol Supplement 96

Shlosberg D, Benifla M, Kaufer D, Friedman A. Blood-brain barrier breakdown as a therapeutic target in traumatic brain injury. Nat Rev Neurol. 2010; 6(7):393–403. [PubMed: 20551947]

Shue E, Carson-Walter E, Liu Y, Winans B, Ali Z, Chen J, Walter K. Plasmalemmal vesicle associated protein-1 (PV-1) is a marker of blood-brain barrier disruption in rodent models. BMC Neuroscience. 2008; 9(1):29. [PubMed: 18302779]

Simionescu M, Popov D, Sima A. Endothelial transcytosis in health and disease. Cell and Tissue Research. 2009; 335(1):27–40. [PubMed: 18836747]

Stan R-V, Marion K, Palade GE. PV-1 is a component of the fenestral and stomatal diaphragms in fenestrated endothelia. Proceedings of the National Academy of Sciences of the United States of America. 1999; 96(23):13203–13207. [PubMed: 10557298]

Sun Y, Hu G, Zhang X, Minshall RD. Phosphorylation of Caveolin-1 Regulates Oxidant–Induced Pulmonary Vascular Permeability via Paracellular and Transcellular Pathways. Circulation Research. 2009; 105(7):676–685. [PubMed: 19713536]

Sun Y, Wang J, Wu X, Xi C, Gai Y, Liu H, Yuan Q, Wang E, Gao L, Hu J, Zhou L. Validating the incidence of coagulopathy and disseminated intravascular coagulation in patients with traumatic brain injury – analysis of 242 cases. British Journal of Neurosurgery. 2011; 25(3):363–368. doi:doi:10.3109/02688697.2011.552650. [PubMed: 21355766]

Tran HT, LaFerla FM, Holtzman DM, Brody DL. Controlled cortical impact traumatic brain injury in 3×Tg-AD mice causes acute intra-axonal aAmyloid-β accumulation and independently accelerates the development of Tau abnormalities. The Journal of Neuroscience. 2011; 31(26):9513–9525. [PubMed: 21715616]

Tyagi N, Roberts AM, Dean WL, Tyagi SC, Lominadze D. Fibrinogen induces endothelial cell permeability. Molecular & Cellular Biochemistry. 2008; 307(1–2):13–22. [PubMed: 17849175]

Wang X, Jung J, Asahi M, Chwang W, Russo L, Moskowitz MA, Dixon CE, Fini ME, Lo EH. Effects of matrix metalloproteinase-9 gene knock-out on morphological and motor outcomes after traumatic brain injury. The Journal of Neuroscience. 2000; 20(18):7037–7042. [PubMed: 10995849]

Wei E, Hamm R, Baranova A, Povlishock J. The long-term microvascular and behavioral consequences of experimental traumatic brain injury after hypothermic intervention. Journal of Neurotrauma. 2009; 26(4):527–537. [PubMed: 19245307]

Yamaguchi M, Jadhav V, Obenaus A, Colohan A, Zhang JH. Matrix Metalloproteinase Inhibition Attenuates Brain Edema in An in Vivo Model of Surgically-Induced Brain Injury. Neurosurgery. 2007; 61(5):1067–1076. 1010.1227/1001.neu.0000303203.0000307866.0000303218. [PubMed: 18091283]

Yu J, Bergaya S, Murata T, Alp IF, Bauer MP, Lin MI, Drab M, Kurzchalia TV, Stan RV, Sessa WC. Direct evidence for the role of caveolin-1 and caveolae in mechanotransduction and remodeling of blood vessels. Journal of Clinical Investigation. 2006; 116(5):1284. [PubMed: 16670769]

Zhang R, Yang D, Zhou C, Cheng K, Liu Z, Chen L, Fang L, Xie P. β-Actin as a loading control for plasma-based Western blot analysis of major depressive disorder patients. Analytical Biochemistry. 2012; 427(2):116–120. doi:http://dx.doi.org/10.1016/j.ab.2012.05.008. [PubMed: 22617797]

Zlokovic BV, Griffin JH. Cytoprotective protein C pathways and implications for stroke and neurological disorders. Trends in Neurosciences. 2011; 34(4):198–209. doi:http://dx.doi.org/10.1016/j.tins.2011.01.005. [PubMed: 21353711]

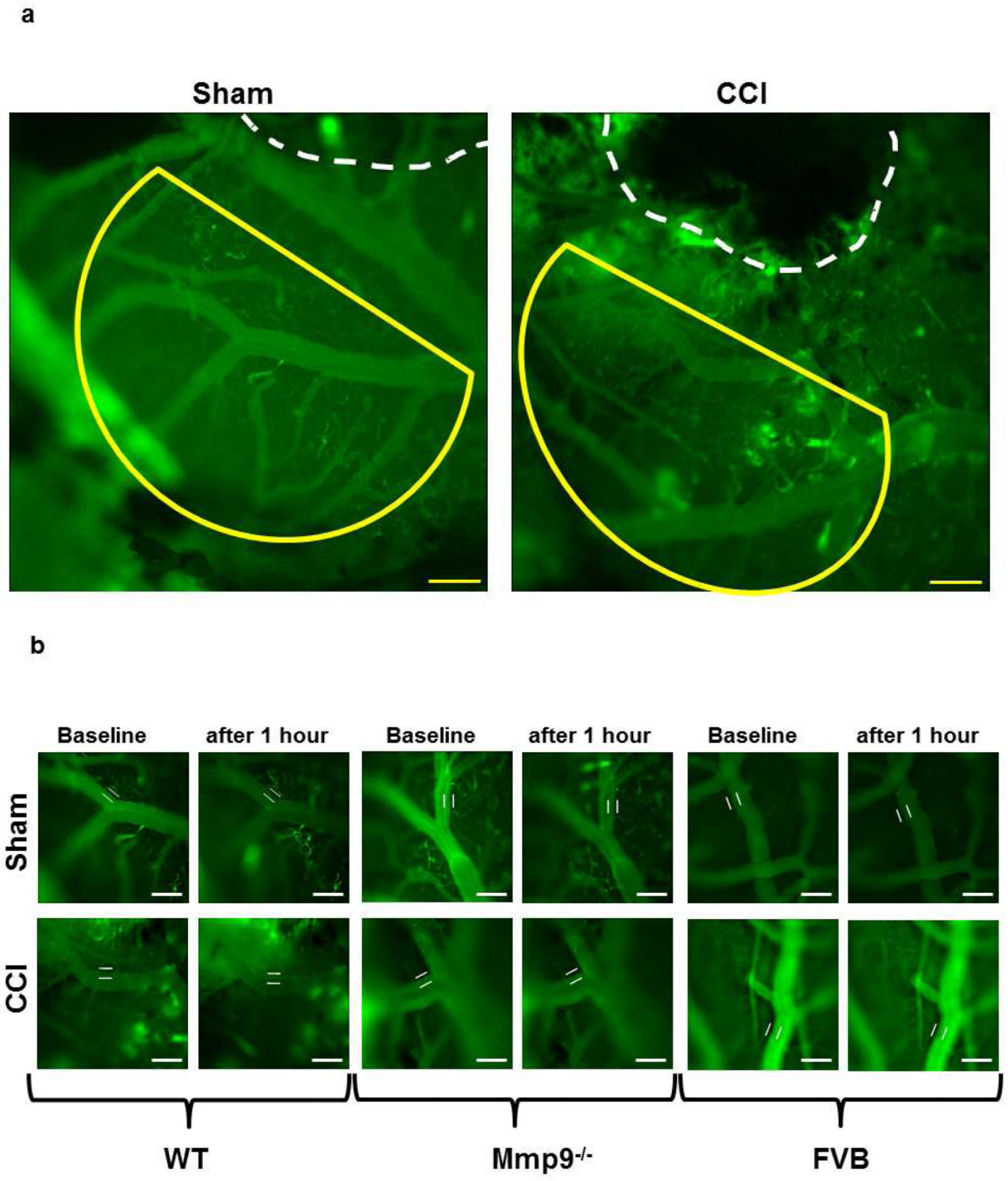

c

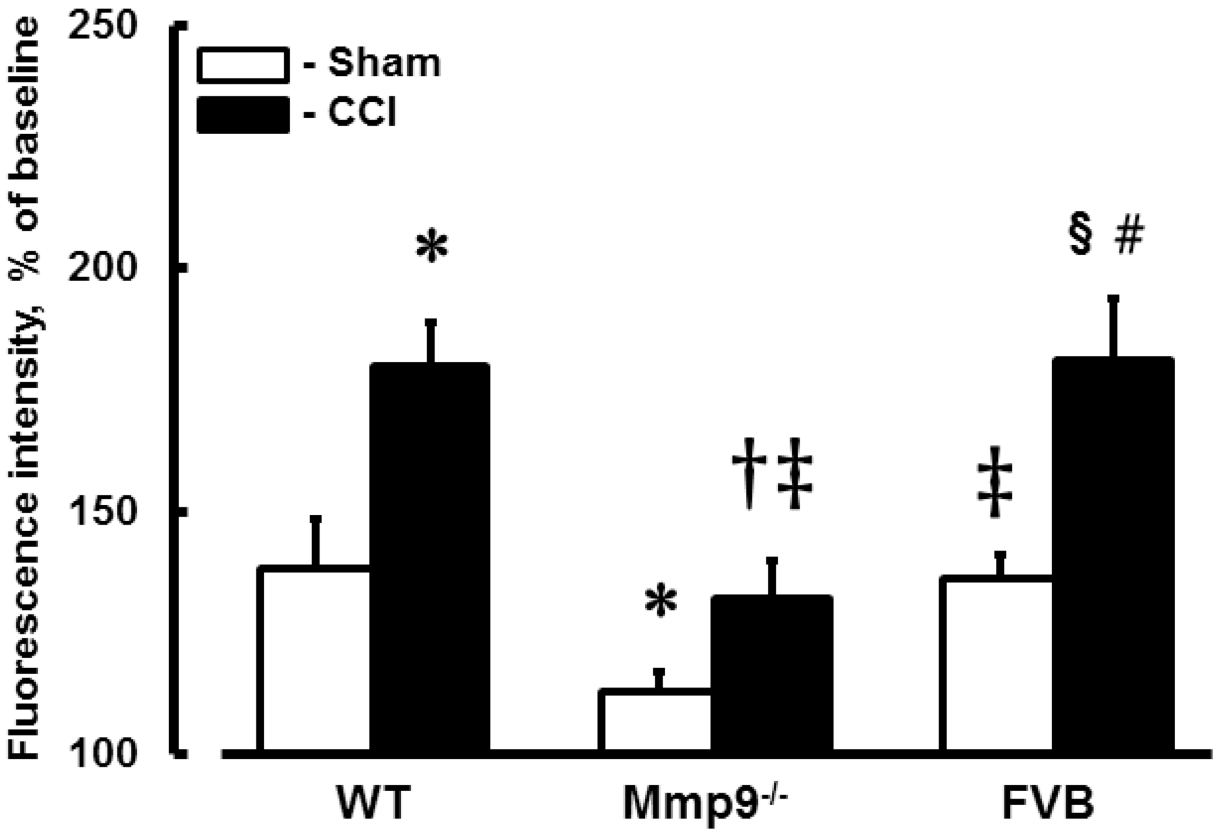

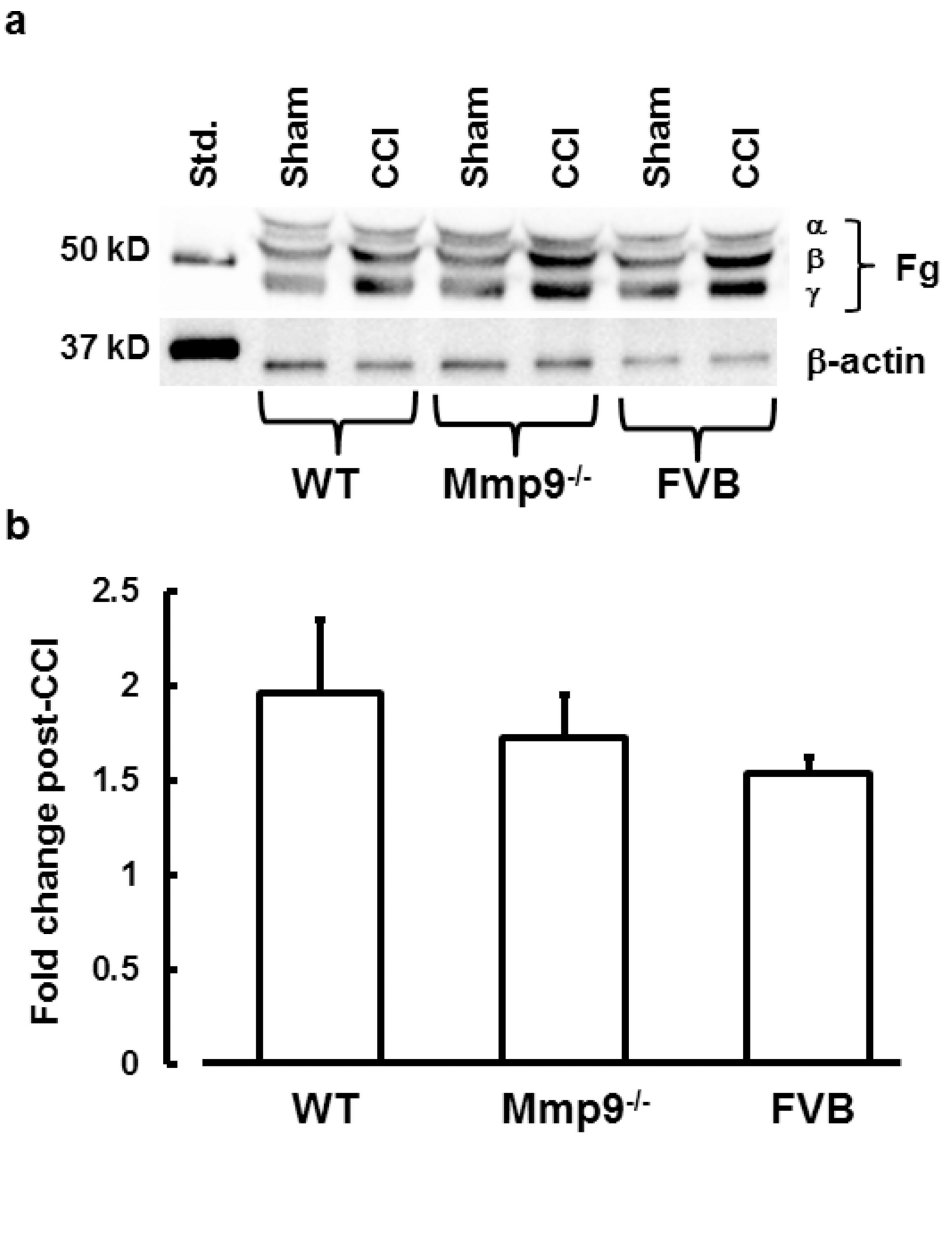


inset

**Fig. 1. Macromolecular leakage of mouse pial venules 14 days after CCI**

a) Examples of observed area (Yellow line) away from the cranial window in Sham-injured mice (left) and the injured area 14 days after CCI (right). Yellow line outlines the area away from the injury where the pial venular leakage was assessed.

*Notes*: practically no injury in sham-injured brain. Small white lines inside and outside of a vessel are Line Profile probes. Objective - 4×. Bar = 160 μm.

b) Example images of FITC-BSA leakage from pial venules in pericontusional area. Bar = 50 μm.

c) Summary of changes in FITC-BSA leakage in C57B/J6 (wild type, WT), MMP-9 gene knockout ($Mmp9^{-/-}$), and FVB mice. Microvascular leakage was assessed by ratio of fluorescence intensity of FITC-BSA along the digital Line Profile probe (LPP) placed

outside of the observed vessel to that mastered along the LPP placed inside the corresponding vascular segment.

Two-way ANOVA indicates significant main effects of genotype, CCI, and interaction. Post-Hoc analysis indicates differences at $P<0.05$ for all: * - vs. WT-Sham, † - vs. WT-CCI, ‡ - vs. $Mmp9^{-/-}$-Sham, § - vs. FVB-Sham, # - vs. $Mmp9^{-/-}$-CCI; n=6

*Inset*: Plasma levels of Fg (α, β, and γ chains) (A) and summary (B) of its changes in plasma samples from WT, $Mmp9^{-/-}$, and FVB mice after sham-injury or CCI are presented. Results of analyses show fold-increase in plasma level of Fg in mice after CCI. A total of 10 μg protein was placed in each well of the SDS gel.

One-way ANOVA showed no significant difference between the groups. n=3 per group

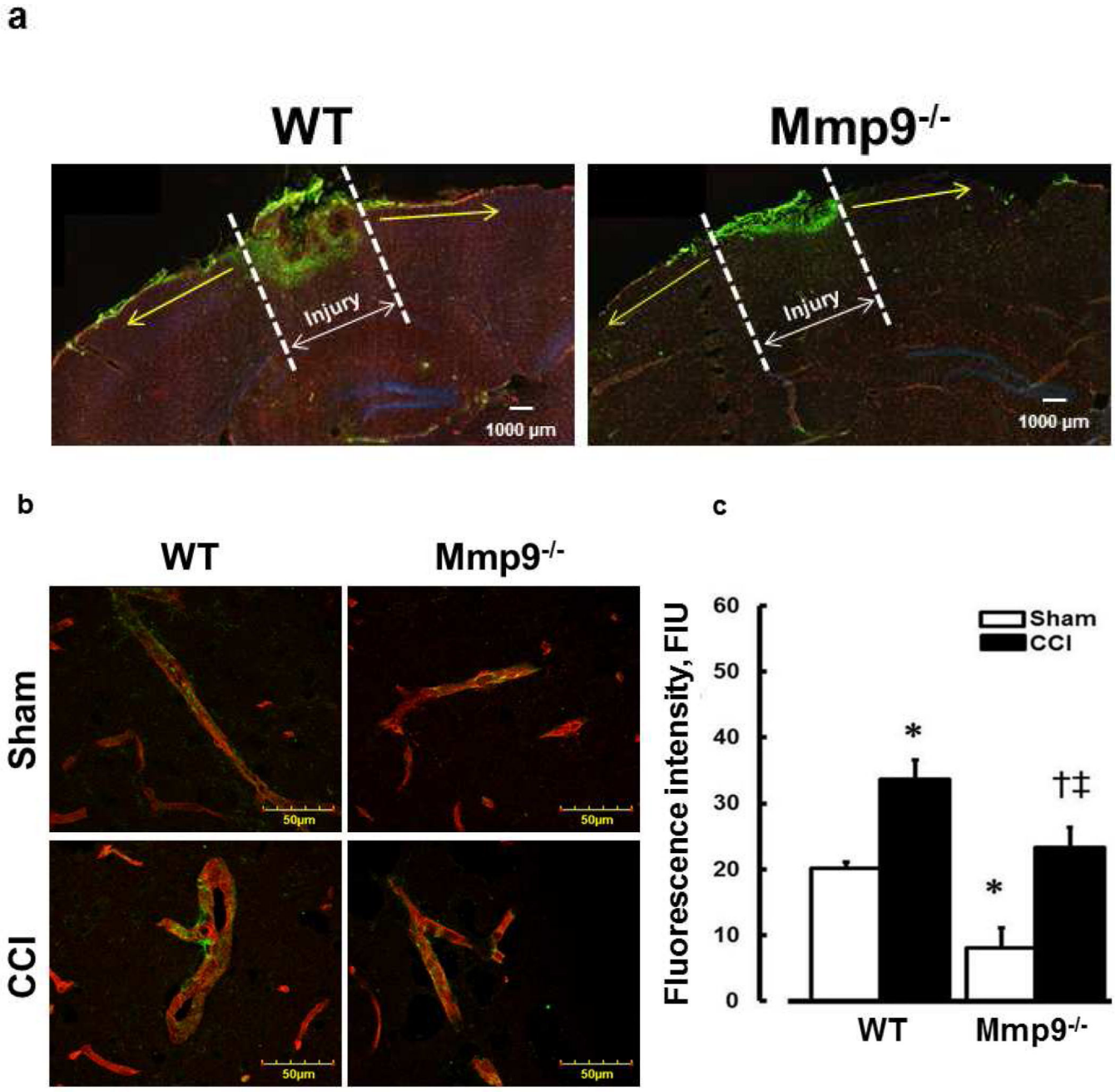


**Fig. 2. Increased expression of intercellular adhesion molecule-1 (ICAM-1) in mouse brain cortical vessels 14 days after CCI**

a) Examples of brain samples from WT and Mmp9$^{-/-}$ mice cryosections in coronal plane through the injury area. Arrows indicate direction where changes in pial microvessels located at least 200 μm away from the injury (dashed line) were observed. The brain microvessels located further than 2000 μm from the injury area and dipper than 200 μm from brain surface were not observed. This is true for all co-immunoprecipitation experiments (Figs. 2 – 6). *Note*: Green fluorescence indicates deposition of Fg after injury, which is visible less in Mmp9$^{-/-}$ mice than that in WT mice.

b) Examples of vessel images obtained from sham-injured (upper row) and contused (CCI, lower row) WT (first column) and MMP-$9^{-/-}$ (second column) mice. Expression of ICAM-1 (green) on the LEA (red)-labeled endothelial surface of a vessel.
c) Summary of ICAM-1 expression in WT and $Mmp9^{-/-}$ mice after sham injury and CCI. Values are expressed per unit length of a vessel segment. Two-way ANOVA indicates significant main effects of genotype and CCI, but no interaction. Post-hoc analysis indicates differences at $P<0.05$ for al: *-vs. WT-Sham, †-vs. WT-CCI, ‡-vs. ($Mmp9^{-/-}$)-Sham; n=4 per group.

a

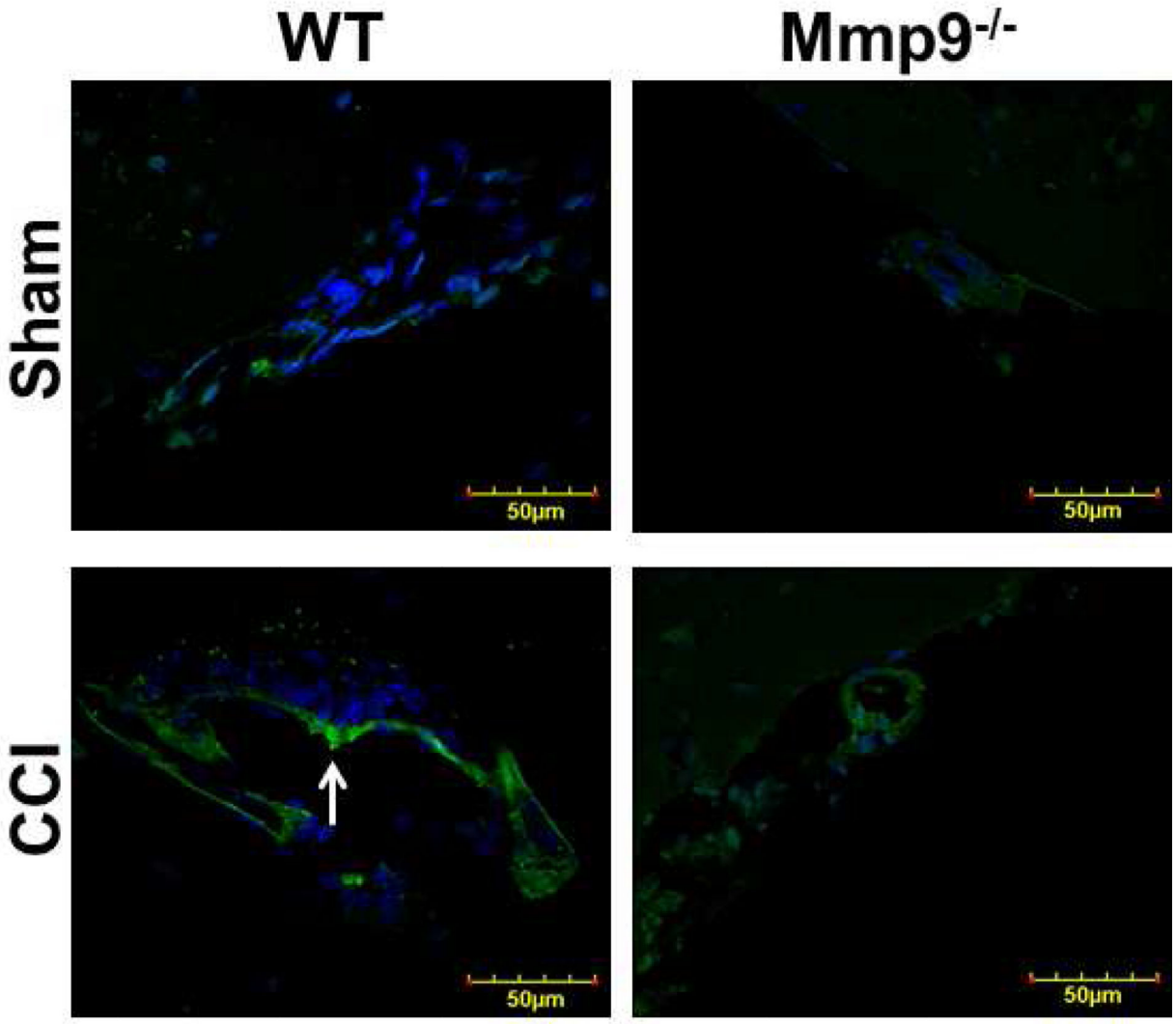

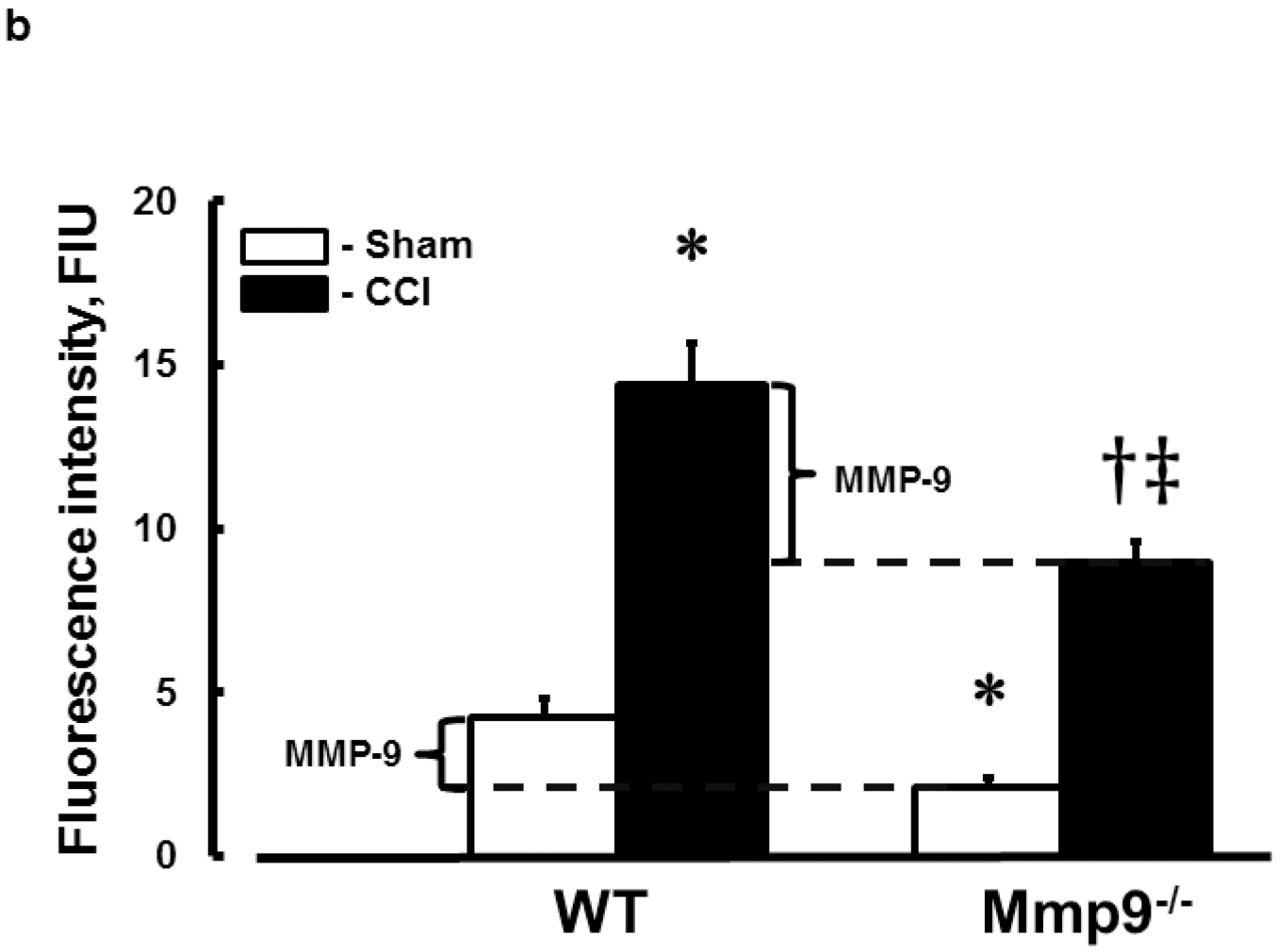


**Fig. 3. Increased activity of metalloproteinase-9 (MMP-9) in mouse brain cortical vessels after CCI**

a) Examples of vessel images in samples obtained from wild type (WT; first column) and MMP-9 gene knockout ($Mmp9^{-/-}$; second column) mice after sham injury (sham, first row) and cortical contusion injury (CCI, second row). MMP-9 activity was assessed by in-tissue zymography assessing fluorescence intensity (green) along the pial vascular segment. DAPI-labeled cellular nuclei are shown in blue.

b) Summary of fluorescence intensity changes in brain vessels after sham-injury or CCI. Differences between values of MMPs activity in sham-operated and post-CCI WT and $Mmp9^{-/-}$ mice indicate activities of MMP-9 in WT mice (shown with brackets). One-way ANOVA indicates differences at $P<0.05$ for all: *-vs. WT-Sham, †-vs. WT-CCI, ‡-vs. ($Mmp9^{-/-}$)-Sham; n=4 per group

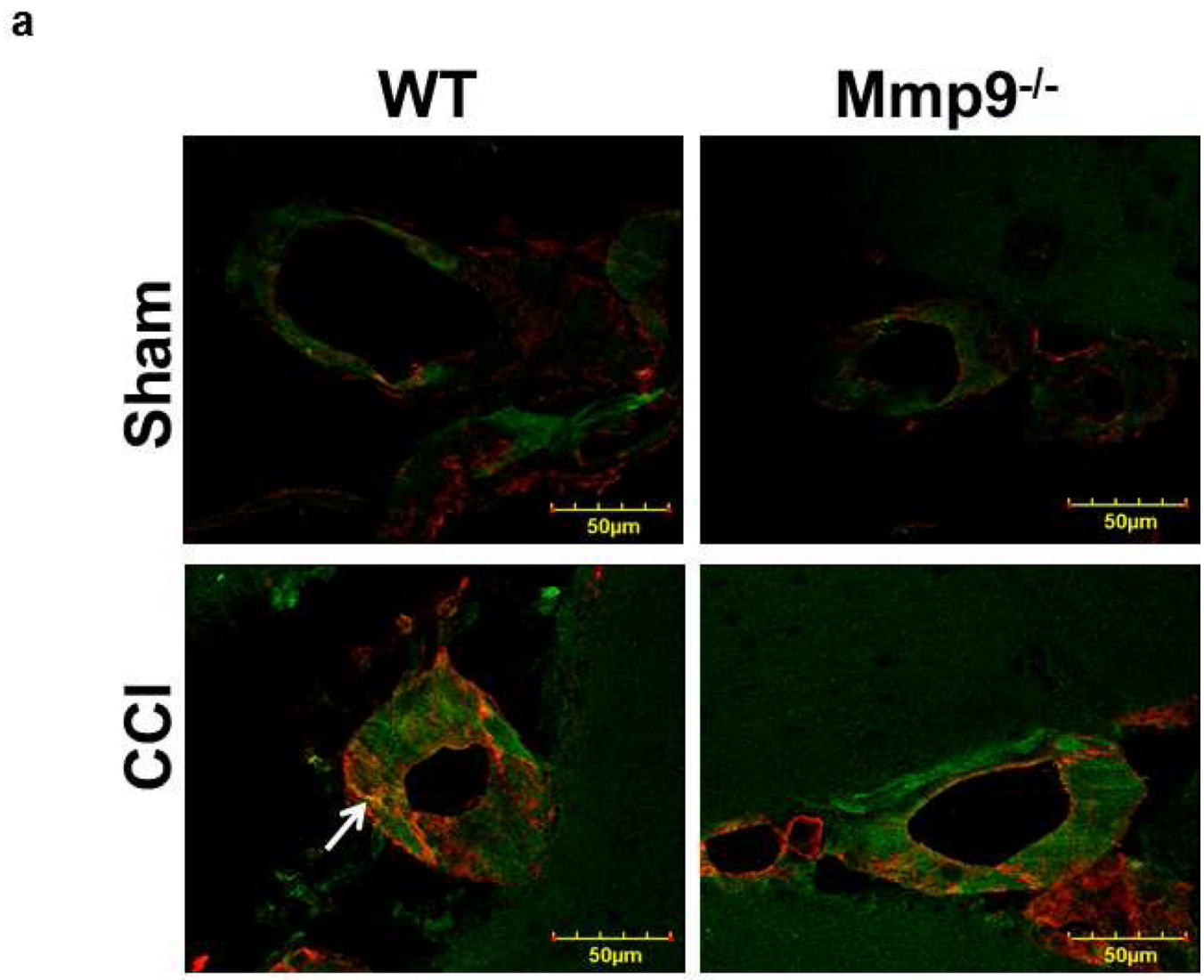

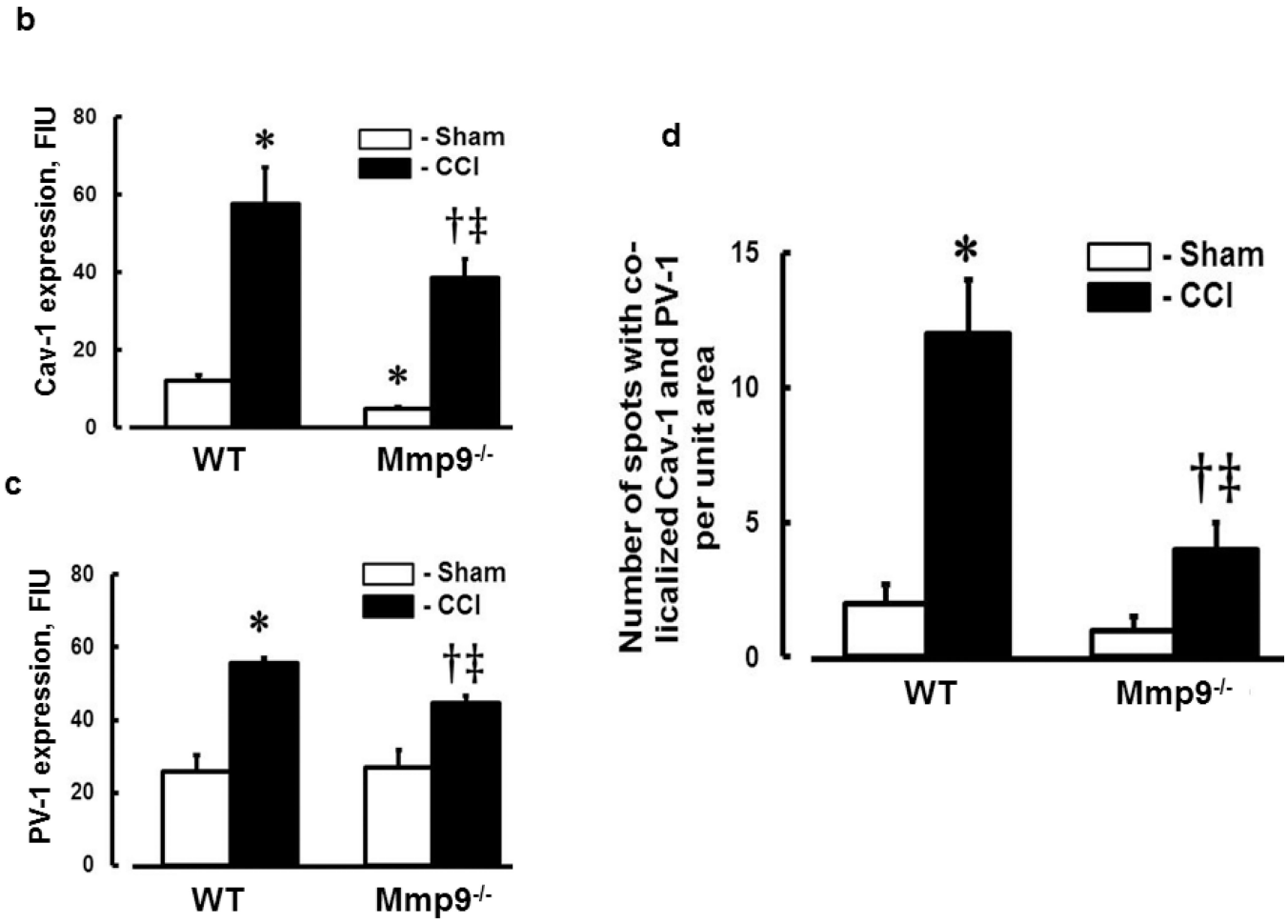


**Fig. 4. Increased formation of caveolae in mouse cortical vessels 14 days after CCI**

a) Examples of vessel images in samples obtained from wild type (WT; first column) and MMP-9 gene knockout ($Mmp9^{-/-}$; second column) mice after sham injury (sham, first row) and cortical contusion injury (CCI, second row). Caveolae (yellow), indicated by white arrow, is defined as co-localization of Cav-1 (red) and PV-1 (green) in cortical vessels.

b) Summary of Cav-1 expression in cortical vessels of WT and $Mmp9^{-/-}$ mice after sham-injury or CCI. Two-way ANOVA indicates significant main effects of genotype and CCI, but no interaction.

c) Summary of PV-1 expression in cortical vessels of WT and $Mmp9^{-/-}$ mice after sham-injury or CCI. Two-way ANOVA indicates significant main effects of genotype and CCI, but no interaction.

d) Summary of Cav-1 and PV-1 co-localization in cortical vessels of WT and $Mmp9^{-/-}$ mice after sham-injury or CCI. Two-way ANOVA indicates significant main effects of genotype, CCI, and interaction.

Post-hoc analyses indicate differences at $P < 0.05$ for all: * - vs. WT-Sham, †- vs. WT-CCI, ‡- vs. ($Mmp9^{-/-}$)-Sham; n=6 per group.

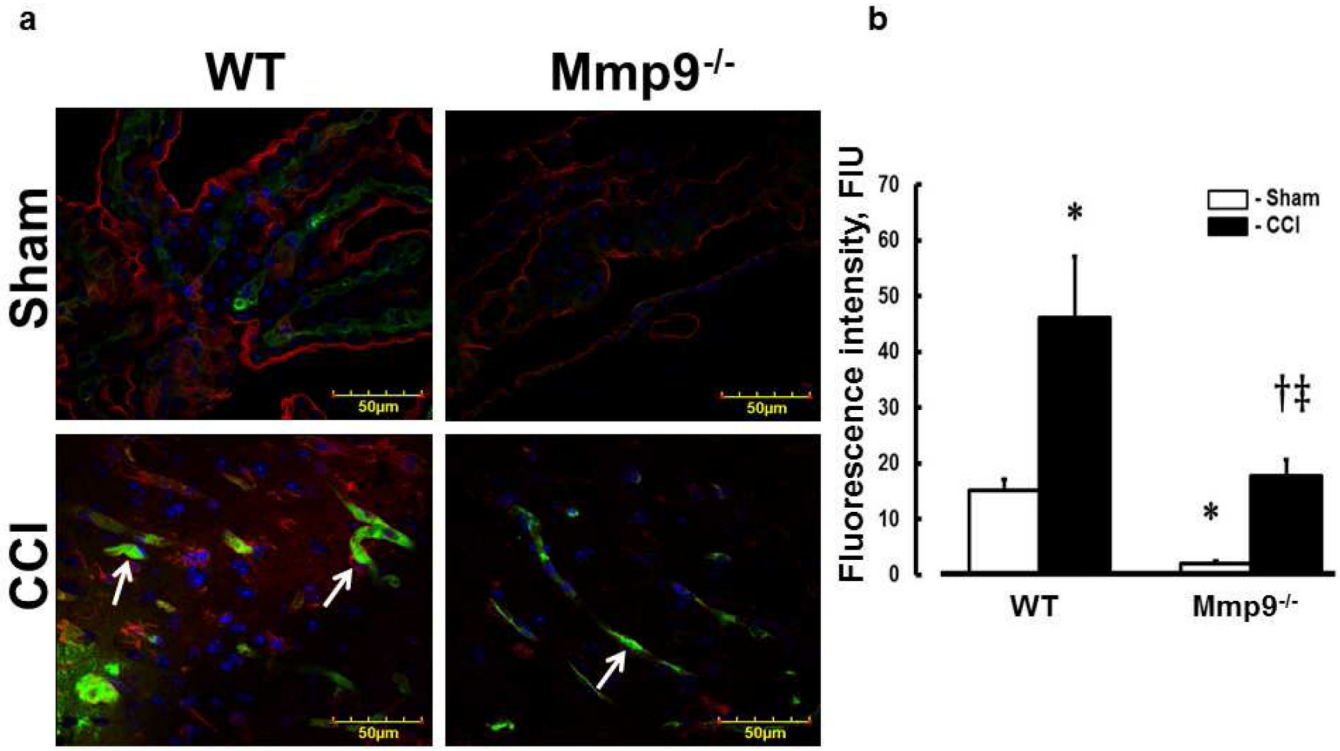


**Fig. 5. Increased phosphorylation of Cav-1 (pCav-1) in mouse brain cortical vessels 14 days after CCI**

a) Examples of vessel images in samples obtained from wild type (WT; first column) and MMP-9 gene knockout ($Mmp9^{-/-}$; second column) mice after sham injury (sham, first row) and cortical contusion injury (CCI, second row). Phosphorylated Cav-1 identified by green color (indicated with arrows) shown in LEA (red)-labeled brain cortical vessels. Cell nuclei are shown in blue (DAPI).

b) Summary of Cav-1 phosphorylation in cortical vessels of WT and $Mmp9^{-/-}$ mice after sham-injury or CCI. Two-way ANOVA indicates significant main effects of genotype and CCI, but not interaction. Post-hoc analysis indicates differences at $P < 0.05$ for all: * - vs. WT-Sham, †- vs. WT-CCI, ‡- vs. $Mmp9^{-/-}$- Sham; n=3 per group.

**a**

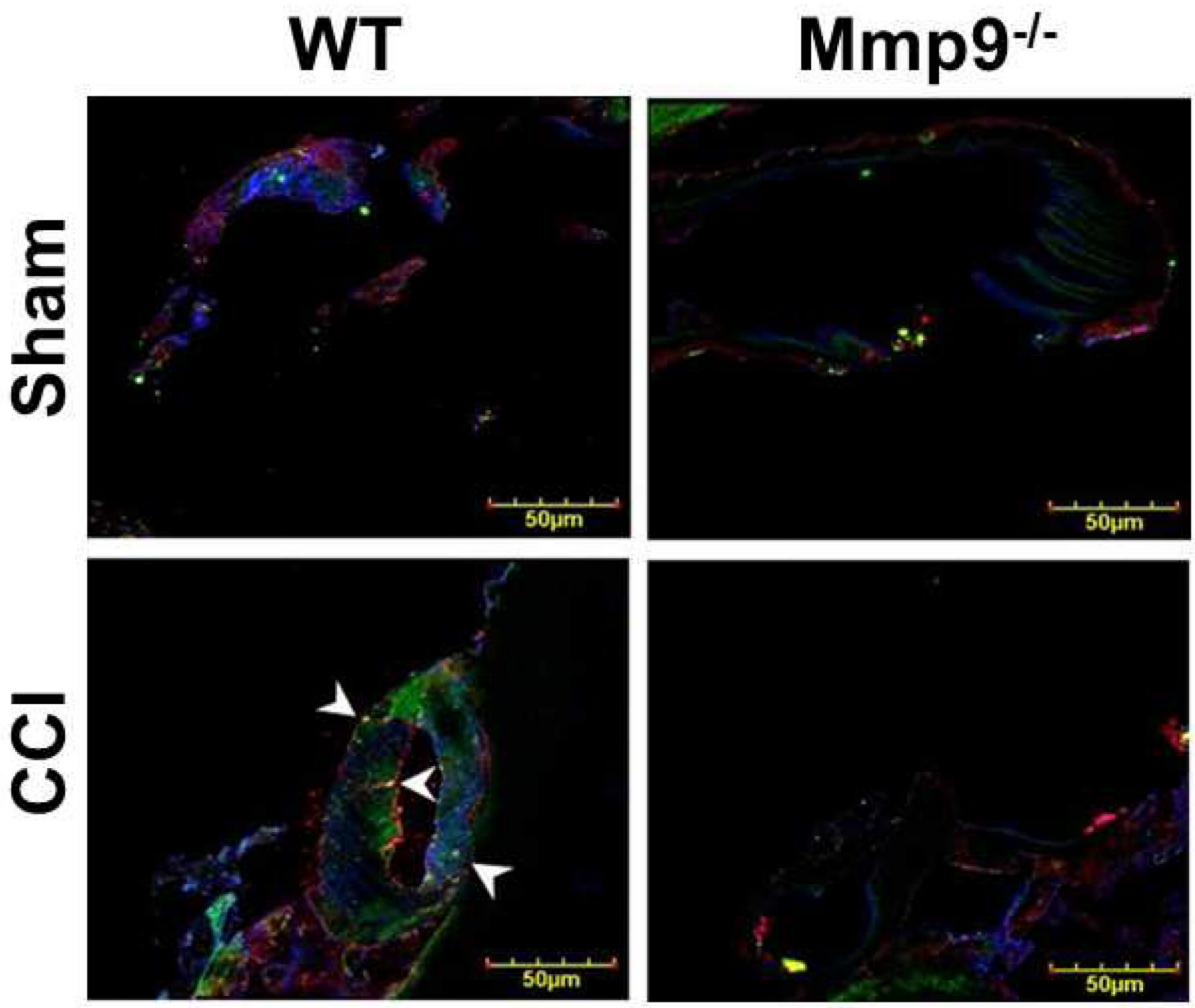

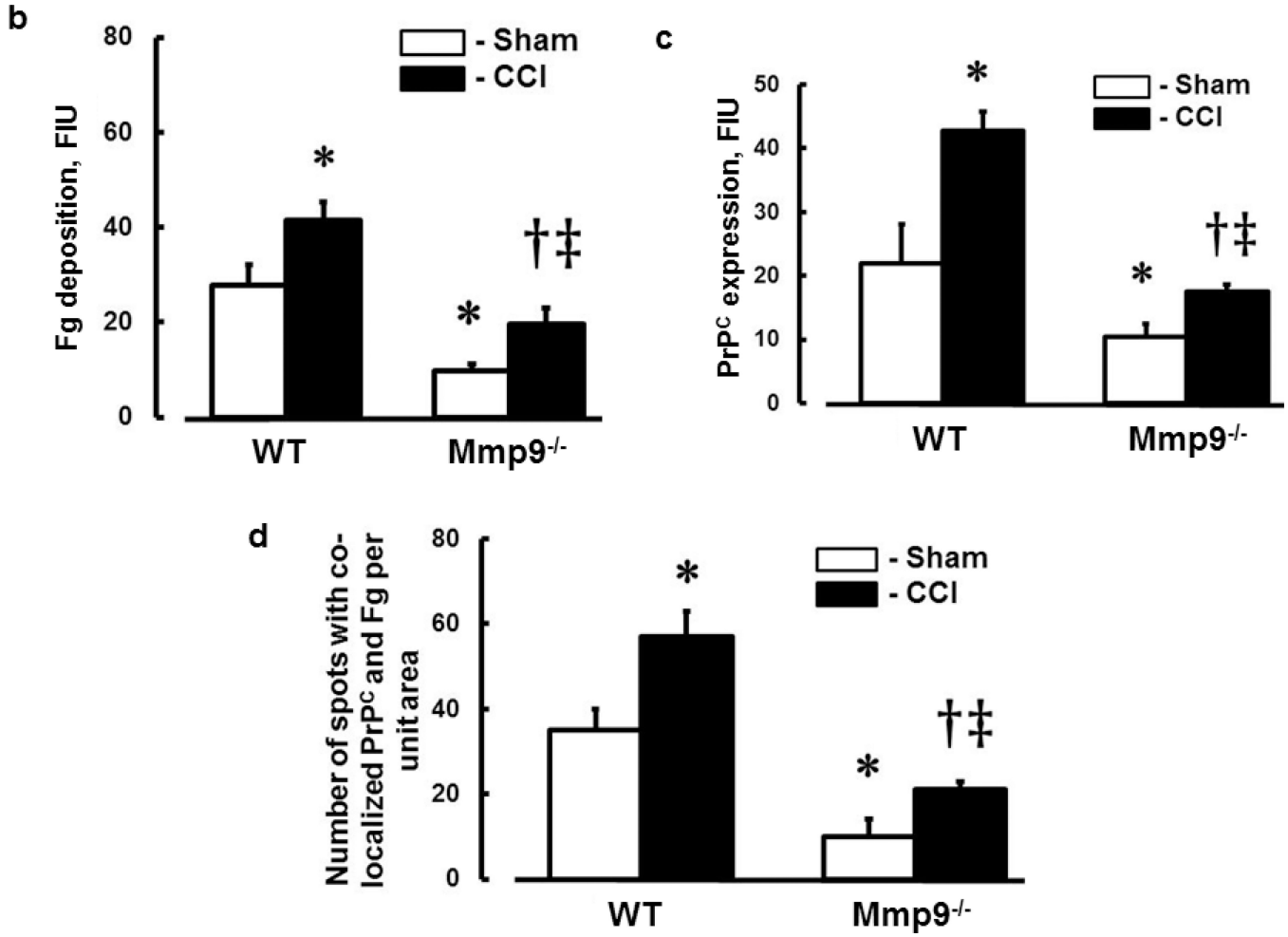


**Fig. 6. Increased deposition of fibrinogen (Fg) and formation of Fg and cellular prion protein ($PrP^C$) complex in mouse brain cortical vessels 14 days after CCI**

a) Examples of vessel images in samples obtained from wild type (WT; first column) and MMP-9 gene knockout ($Mmp9^{-/-}$; second column) mice after sham injury (sham, first row) and cortical contusion injury (CCI, second row). Deposition of Fg (red) and $PrP^C$ (green) and formation Fg-$PrP^C$ complex (yellow, shown with arrowheads) in mouse brain vessels was increased after CCI compared to that in Sham-injured mice. LEA is shown in blue (pseudocolor).

b) Summary of Fg deposition changes (defined by fluorescence intensity) in brain vessels after sham-injury or CCI. Two-way ANOVA indicates significant main effects of genotype and CCI, but no interaction.

c) Summary of $PrP^C$ deposition changes (defined by fluorescence intensity) in brain vessels after sham-injury or CCI. Two-way ANOVA indicates significant main effects of genotype and CCI, but no interaction.

d) Summary of Fg-$PrP^C$ complex formation defined by number of spots of co-localized Fg and $PrP^C$ in brain samples after sham-injury or CCI. Two-way ANOVA indicates significant main effects of genotype, CCI, and interaction.

Post-hoc analyses indicate differences at $P < 0.05$ for all: * - vs. WT-Sham, † - vs. WT-CCI, ‡- vs. $Mmp9^{-/-}$- Sham; n=4 per group.

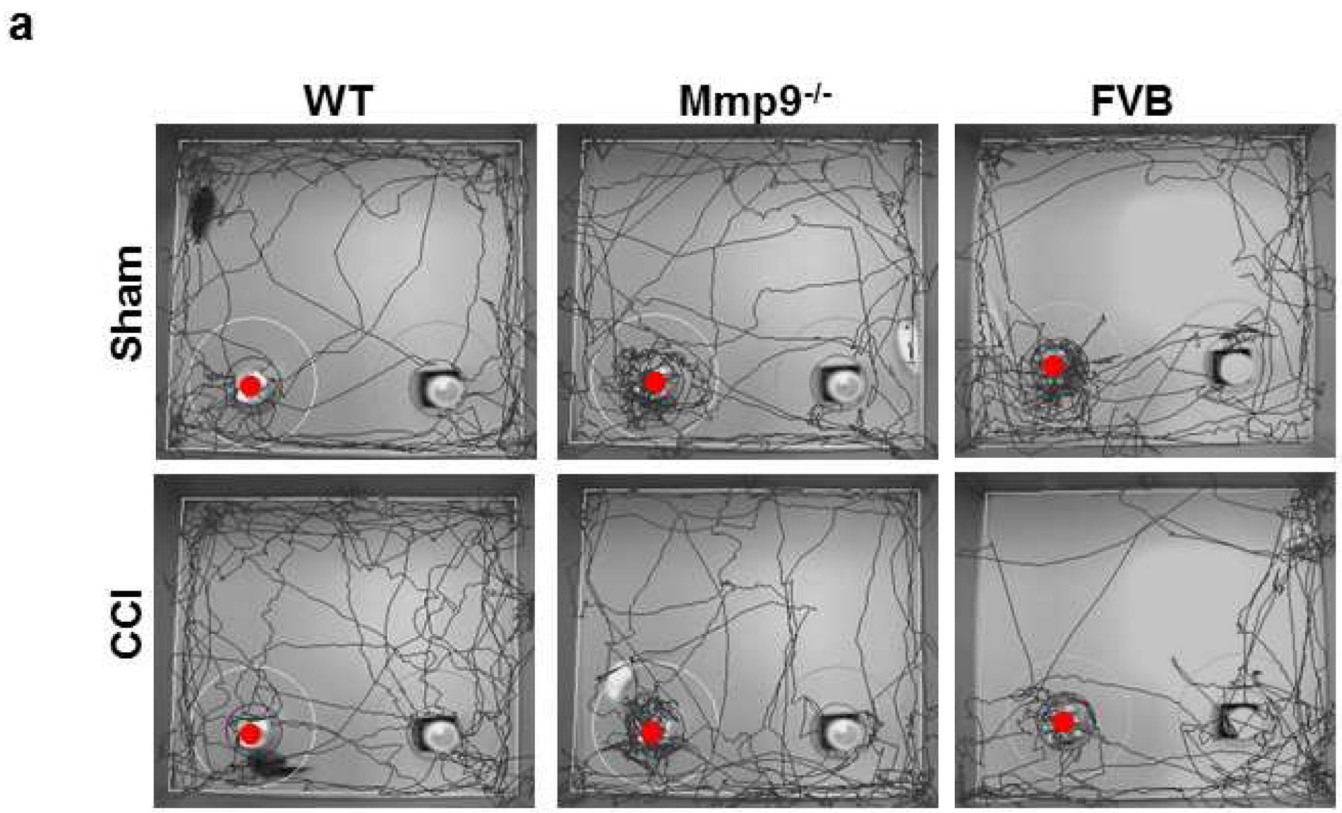

b

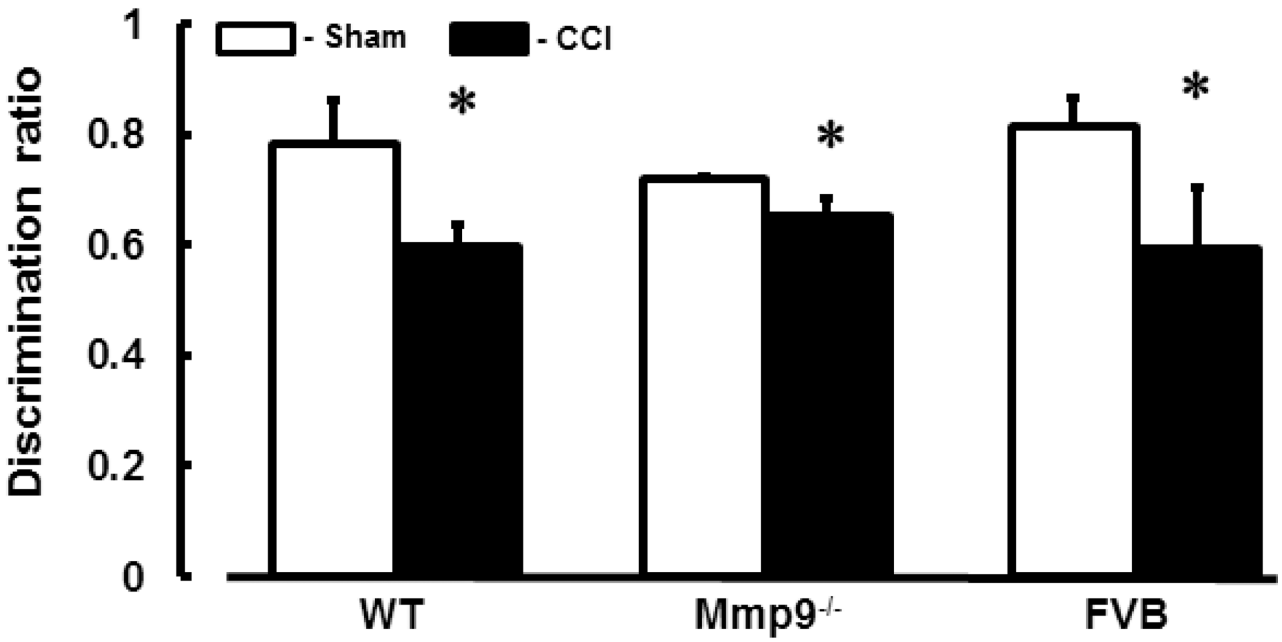

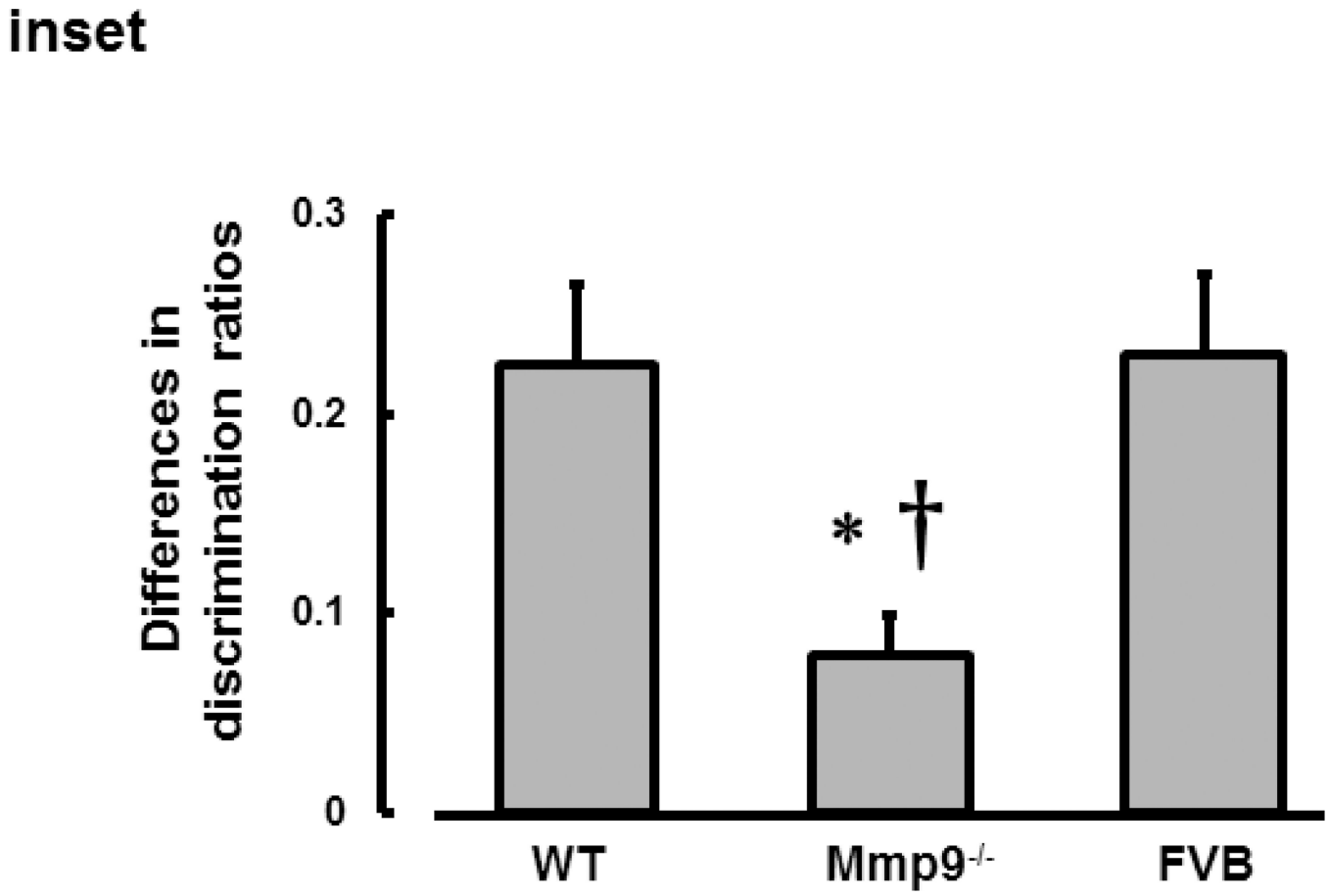


**Fig. 7. Short-term memory of mice after cortical contusion injury**

a) Examples of movement traces for wild type (WT, first column), MMP-9 gene knockout ($Mmp9^{-/-}$, second column) and FVB (third column) mice after sham injury (sham, upper row) or cortical contusion injury (CCI, lower row). Short-term memory in mice was assessed by novel object recognition test (NORT). Lower discrimination ratio indicates impaired short-term memory. *Note*: The red dot indicates the new object.

b) Summary of discrimination ratios obtained by NORT for WT, $Mmp9^{-/-}$, and FVB mice after sham injury or CCI. Two-way ANOVA indicates no significant main effects of genotype, CCI, and interaction. Post-hoc analysis indicates difference at $P < 0.05$: * - vs. Sham; n=22

*Inset*: The difference in discrimination ratios between sham-operated and CCI mice was significantly less in $Mmp9^{-/-}$ mice than that in WT or FVB mice. The analysis was done with one-way ANOVA: $P < 0.05$ for both, * - vs. Sham †- vs. FVB.

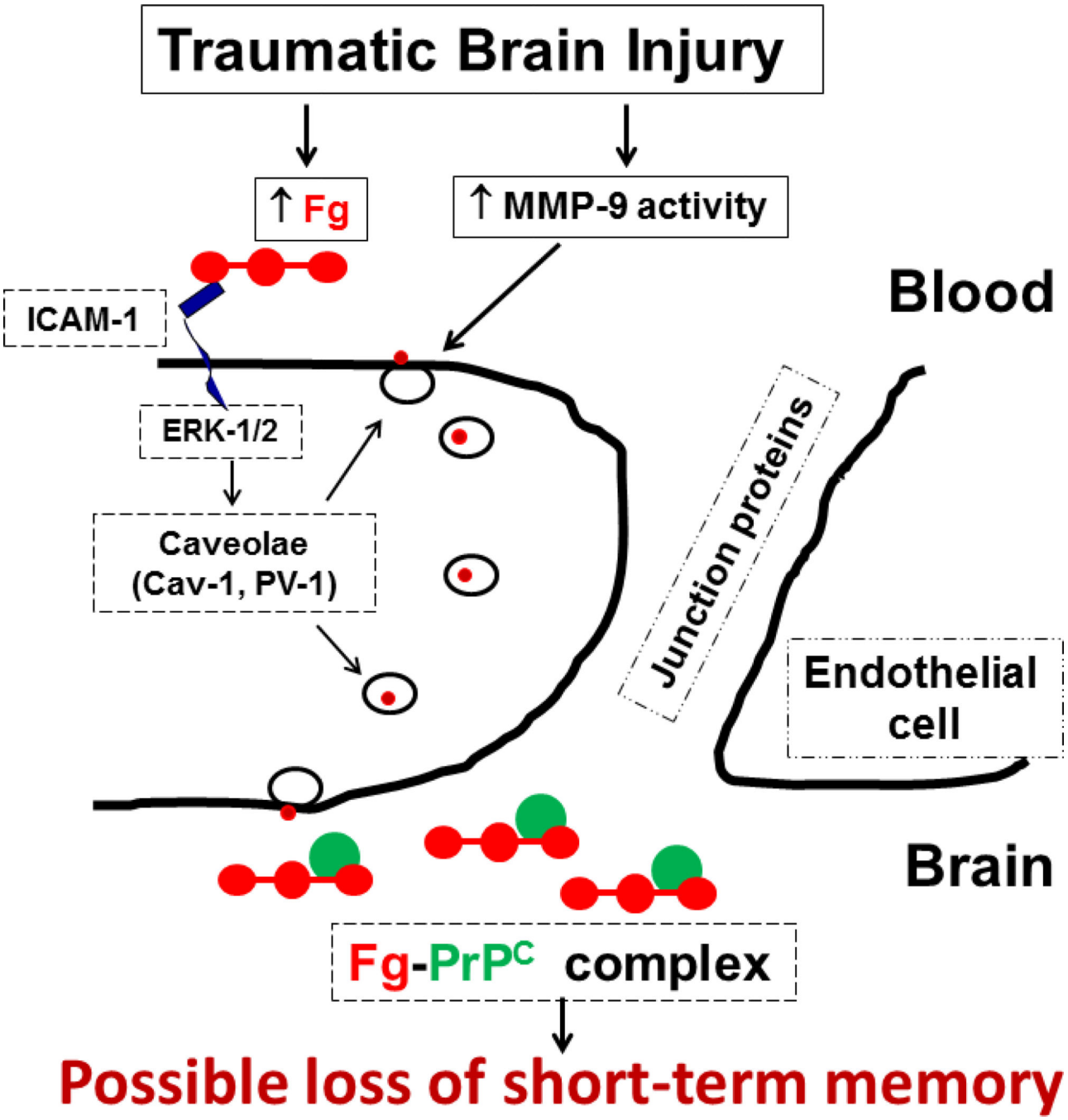


**Fig. 8. Schematic representation of a possible mechanism involved in traumatic brain injury (TBI)-induced formation of fibrinogen-cellular prion protein (Fg-PrP$^{C}$) complex and the resultant short-term memory impairment**

TBI increases activity of matrix metalloproteinase-9 (MMP-9) and leads to an increase in blood level of Fg. The latter increases blood viscosity and results in activation of endothelial cells (ECs), and as a result, activation of intercellular adhesion molecule-1 (ICAM-1) (Muradashvili and Lominadz 2013). This leads to an enhanced binding of Fg to endothelial ICAM-1 and activates extracellular signal-regulated kinases 1 and 2 (ERK-1/2) (Sen et al. 2009). Activation of ERK-1/2 most likely leads to phosphorylation of caveolin-1 (pCav-1),

which is involved formation of functional caveolae (in the present study, defined by co-localization of Cav-1 and plasmalemmal vesicle associated protein-1, PV-1) (Muradashvili and Lominadz 2013). In addition, activation of MMP-9 may be involved in caveolae function (Phillips and Birnby 2004). Increased caveolar transcytosis results in accumulation of Fg in subendothelial matrix and leads to formation of Fg-$PrP^C$ complex. This can result in impairment of short-term memory.